STEREOSCOPIC SURFACE INTERPOLATION FROM ILLUSORY CONTOURS

BRITTNEY HARTLE

A THESIS SUBMITTED TO THE FACULTY OF GRADUATE STUDIES IN PARTIAL FULFILLMENT OF THE REQUIREMENTS FOR THE DEGREE OF MASTER OF ARTS

GRADUATE PROGRAM IN PSYCHOLOGY
YORK UNIVERSITY
TORONTO, ONTARIO

September 2016

Abstract

Stereoscopic Kanizsa figures are an example of stereoscopic interpolation of an illusory surface. In such stimuli, luminance-defined disparity signals exist only along the edges of inducing elements, but observers reliably perceive a coherent surface that extends across the central region in depth. The aim of this series of experiments was to understand the nature of the disparity signal that underlies the perception of illusory stereoscopic surfaces. I systematically assessed the accuracy and precision of suprathreshold depth percepts using a collection of Kanizsa figures with a wide range of 2D and 3D properties. For comparison, I assessed similar perceptually equated figures with luminance-defined surfaces, with and without inducing elements. A cue combination analysis revealed that observers rely on ordinal depth cues in conjunction with stereopsis when making depth judgements. Thus, 2D properties (e.g. occlusion features and luminance relationships) contribute rich information about 3D surface structure by influencing perceived depth from binocular disparity.

Table of Contents

Chapter 1

Introduction

1.1. Illusory Contours

Illusory contours occur when boundaries are perceived in an image in the absence of a corresponding luminance gradient. Schumann (1900) first described these contours as 'subjective' because they do not exist in the physical stimulus, only in the observer's interpretation of it. He argued that the visual system detects features in these figures that trigger fundamental perceptual phenomena, resulting in the perception of contours in the absence of luminance, texture, or colour boundaries. Studies of illusory phenomenon often focus on illusory boundaries generated from luminance discontinuities, such as edges or line terminations (Lesher, 1995). This type of illusory contour is consistent with a stimulus arrangement in which texture is partially occluded by another region due to equivalent contrast. In this case, the regular alignment of edges or endpoints of the occluded texture creates a percept of an illusory contour. For example, Ehrenstein's figure (1941) is created by line terminations that surround a region of homogeneous luminance; this results in the formation of illusory contours at the end-points that create a boundary around the central region. Abutting line terminations can also create illusory boundaries using a variety of different texture patterns (see Gilliam & Nakayama, 2002; Kanizsa, 1974). Examples of illusory contours can also be seen in works of art. Ellsworth Kelly completed a series of paintings in the 1950s that use line terminations to generate illusory contours that emphasize the boundaries of sparse objects (Shapley, 1996). While illusory boundaries can be created under a wide range of conditions, the most well-known examples are those created by Kanizsa (1955) (Figure 1.1). Many variants of two-dimensional (2D) Kanizsa figures have been used to study the properties of illusory contours and constraints on their formation (Banton &

Levi, 1992; Coren, 1972; Ullman, 1976). These studies have identified several percepts common to Kanizsa figures, i) the presence of definite boundaries between the inducers, ii) depth ordering of the inducers and the central region, and iii) lightness differences between the central region and the background. These phenomena may be seen in Figure 1.1 where illusory boundaries are formed between the four circular inducing elements that results in the percept of a rectangular surface positioned between the observer and the four disks. Studies of depth perception in 2D Kanizsa figures have consistently shown that the central region is perceived as closer to the viewer than the inducing elements (Bradley & Dumais, 1984; Coren, 1972; Coren & Porac, 1983). In Kanizsa's figures (and many subsequent modifications), a complete square is seen even though this shape is specified only by the relative position of the inducing elements (i.e. their geometric arrangement). The illusory boundaries generated by these Kanizsa configurations are perceptually similar to luminance edges in that they: (i) share neural architecture that process luminance-defined edges (Larsson et al., 1999; von der Heydt, Peterhans, & Baumgartner, 1984), (ii) share similar perceptual effects (Paradiso et al., 1989; Smith & Over, 1979; Vogels & Orban, 1987), and (iii) exhibit rivalry with luminance-defined edges (Fahle & Palm, 1991). As outlined below, the perception of illusory boundaries in Kanizsa figures appears to depend on both the local cues to occlusion at the inducing elements as well as global geometric cues.

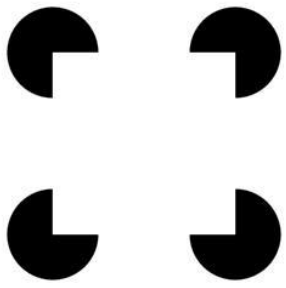

Figure 1.1. Square Kanizsa figure with four high contrast inducing elements.

1.2. Occlusion Geometry

As noted above, the perceived depth order derived from the occlusion geometry in Kanizsa figures plays a key role in creating its illusory boundaries (Coren, 1972; Gillam & Nakayama, 2002; Kellman & Shipley, 1991; Rubin, 2001). When the edge of an occluding surface intersects that of an occluded region, a 2D discontinuity called a junction is formed. For example, in Figure 1.1, the Kanizsa has two regions with visible contour junctions at, (i) the vertices of the central illusory square, and (ii) the tips of the inducing elements. These junctions are points at which the contour has no unique orientation. Previous researchers have investigated the relationship between the structure of these 2D junctions and the perceived geometry of the illusory surface (Anderson & Julesz, 1995; Anderson, 1997; Shipley & Kellman, 1990). In general, the interpolation of 2D illusory boundaries begins and ends at these critical points, and if they are removed, contour interpolation is markedly reduced or eliminated (Shipley & Kellman, 1990)[1]. In Figure 1.1, the interpolation of the illusory boundaries begins and ends at the explicit L-junctions at the tips of the inducing elements. In natural environments, when surfaces belonging to two distinct objects overlap they tend to form a T-junction. These junctions are reliably interpreted by the visual system as a monocular indicator of a depth discontinuity (Helmholtz, 1909). Typically, the top of the T-junction is assigned to the edge of the occluding object and the stem is assigned to the partially occluded object (Nakayama et al., 1989). It has been argued that when interpreting Kanizsa figures, viewers assume that the occluder and background have the same luminance, thus one arm of the T-junction is camouflaged. Thus, although physically this region forms an L-junction it is interpreted as a T-junction. The 2D

[1] There are examples in which two objects are in contact that suggest tangent discontinuities may not be critical for all cases of illusory contour formation (see Tse & Albert, 1998). While these exceptions show that illusory volumes can occur without these discontinuities, they do play a critical role in Kanizsa-like configurations.

geometry at these physical L-junctions is ambiguous, since there are two competing illusory T-junctions that represent two possible positions of an occluding surface (see Figure 1.2). One way to resolve this border-ownership problem is to add a luminance change to define the T-junction as belonging to the outer inducing edge or the illusory square, which changes the perceived depth order of the figure from amodal (i.e. illusory square behind the inducers) to modal (i.e. illusory square in front of inducers) completion (see Figure 3 in Anderson, Singh, & Fleming, 2002). While it has been demonstrated that these junctions play a critical role as local occlusion cues that initiate contour interpolation processes (Rubin, 2001), alone they are not sufficient for contour interpolation (Kellman, Garrigan, & Shipley, 2005). To resolve this border-ownership ambiguity, the visual system can rely on global geometric assumptions (e.g. the geometric relations between adjacent inducing elements).

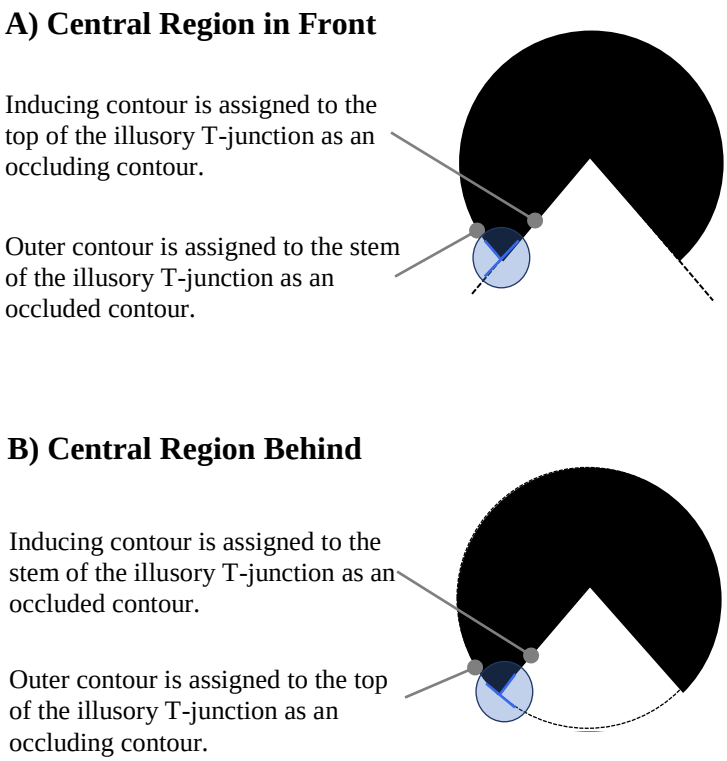

Figure 1.2. An illustration of the two possible depth order configurations in a Kanizsa figure based on the occlusion geometry at the tips of the inducing elements. The illusory T-junctions at the tips of the inducing elements are highlighted in blue. The two configurations depend on which one of the edges that meet at the explicit L-junction is assumed to continue beyond the tip (modified figure from Anderson, Singh, & Fleming, 2002).

One critical global geometric property that enhances the strength of illusory boundaries and facilitates their stability is the collinearity (i.e. alignment) of the inducing edges (Grossberg & Mingolla, 1985). This constraint has been recast as 'relatability' by Kellman and Shipley (1991). They argue that alignment requirements should be considered in terms of 'contour relatability' and that the visual system only interpolates contours that meet particular smoothness constraints and monotonicity (i.e. interpolated contours bend in only one direction). However, while collinearity contributes to the 2D interpolation of smooth connected contours, there is evidence that it is not necessary to initiate the formation of illusory contours (Anderson, 2007;

Gillam, 1987). Furthermore, there are other global/geometric properties (e.g. similarity) that can facilitate the perception of illusory boundaries and influence the trajectory of interpolated contours.

The local occlusion geometry and global geometric cues are used by the visual system to specify border-ownership of the illusory edges in conventional 2D Kanizsa figures. This in turn determines the perceived depth order of the illusory surface and inducing elements (Gillam & Nakayama, 2002; Kogo et al., 2010). The presence of perceived depth order in the illusory surfaces described above is supported by functional imaging studies that demonstrate brain areas related to depth-recognition tasks are consistently activated when observing 2D illusory Kanizsa figures (Mendola et al., 1999).

1.3. Lightness Illusion

The illusory surface elicited by 2D Kanizsa figures is commonly accompanied by a lightness enhancement in the central region that causes the region to appear brighter than the homogeneous background (when dark inducing elements on presented on a light background as in Figure 1.1). Previous research has shown that although lightness illusions do not always occur along with illusory surface percepts (Day, 1987; Dresp, Lorenceau, & Bonnet, 1990; Kogo et al., 2010), when they do occur, illusory boundaries are typically perceived (He & Ooi, 1998; Prazdny, 1983). Further, the quality of the lightness illusion depends on both the presence of the illusory boundaries, and on attributes of the inducing elements, such as their polarity (Matthews & Welch, 1997), and perceived depth order (Kogo et al., 2014). Recently, Kogo et al. (2014) proposed a neurocomputational model in which they suggest that the qualitative depth percepts and lightness enhancement elicited by 2D Kanizsa figures are processed in parallel and integrated to create the occluding illusory surface. The effects of depth order on the perception of

photometric properties in general is well documented (Adelson, 1993; Knill & Kersten, 1991; Wishart, Frisby, & Buckley, 1997), leading researchers to argue that lightness perception is intimately related to depth perception (Gilchrist, 1977; Gilchrist, 1980). For example, there is a strong bias to perceive brighter objects as closer than dim objects (Ashley, 1898; Coules, 1955; Farne, 1977; Kanizsa, 1976; Taylor & Summer, 1945). Regardless of the processing sequence, it is clear that both the geometric layout and the perceived lightness enhancement contribute to the perception of 2D Kanizsa figures. However, it should be noted that because the depth information in these 2D images is qualitative (not quantitative) in nature, observers can only indicate the sign of the depth (e.g. is the surface in front of or behind the inducing elements), not the amount of depth. Three-dimensional (3D) Kanizsa figures can provide a more robust perception of depth by introducing binocular disparity between inducing edges.

1.4. Stereoscopic Kanizsa Figures

A number of investigators have shown that the apparent depth of the illusory surface in Kanizsa figures is greatly enhanced when they are viewed stereoscopically (Carman & Welch, 1992; Ramachandran, 1986; Vreven & Welch, 2001). In some respects, this is not surprising given that one of the primary roles of the stereoscopic system is to identify and interpret surfaces in the environment (Anderson, Singh, & Fleming, 2002; Wilcox & Duke, 2003; Yang & Blake, 1995). However, as illustrated in Figure 1.3, illusory surfaces that extend over regions of uniform luminance represent a special case of stereoscopic surface interpretation (Harris & Gregory, 1973). In Figure 1.3 the vertical inducing edges of the 3D Kanizsa figure are rendered with positional disparity, consistent with the presence of a white foreground surface in 3D space. By manipulating the relative position and orientation of the inducing edges in each eye, dramatic changes can be made to the perceived shape of the 3D illusory surface (for more examples see

Carman & Welch, 1992). The interpretation of the surface in the 3D Kanizsa figure depends on the combined effect of the 2D information described above (occlusion geometry and lightness enhancement), as well as the magnitude of depth defined by binocular disparity. The large regions of homogeneous luminance in these figures pose a challenge to binocular disparity matching, as there are no unique features within this area to guide correspondence (Jones & Malik, 1992).

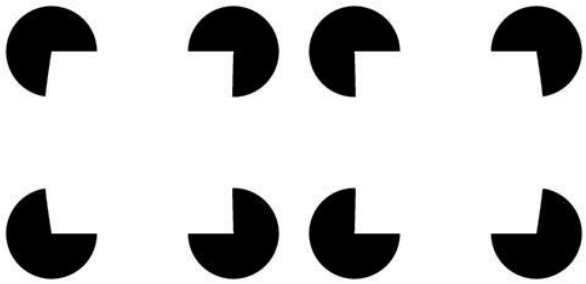

Figure 1.3. A stereopair of a high contrast Kanizsa figure. When stereoscopically cross-fused the disparity information at the inducing elements generate the percept of a 3D crossed-disparity illusory surface in the absence of luminance-defined disparity information within region of homogeneous luminance.

To understand how complete stereoscopic surfaces are formed in 3D Kanizsa figures it is important to consider both the 2D occlusion geometry and 3D (stereoscopic) depth information (Anderson & Julesz, 1995; Ehrenstein & Gillam, 1999). In Figure 1.4, when the two left Kanizsa figures are perceptually cross-fused, the illusory surface bows towards the viewer and occludes the four black inducing elements (i.e. modal completion). However, when the two rightmost Kanizsa figures are cross-fused, the disparity is reversed and the illusory surface appears to extend behind the plane of the four inducing elements. The surface now bows away from the observer, and for some observers, appears as though it is viewed through four circular apertures within an opaque fronto-parallel occluding surface (i.e. amodal completion, see Michotte, 1963). In these 3D Kanizsa configurations, the positional disparity between the vertical inducing edges

combines with the 2D illusory T-junctions present in each monocular image to create stereoscopic illusory T-junctions (Anderson, 2003). When the disparity signal at these junctions is uncrossed (rightmost Kanizsas in Figure 1.4) the 2D occlusion geometry (i.e. 2D T-junctions) and the binocular disparity signal are in conflict. In this case, the 2D illusory boundaries in each monocular image of the stereopair are modal (i.e. the illusory boundaries always occlude the inducing elements), regardless of the disparity signal. Thus, given that the top of the T-junction cannot act as an occluding edge the uncrossed illusory surface is incompatible with the 2D occlusion geometry (Nakayama & Shimojo, 1992).

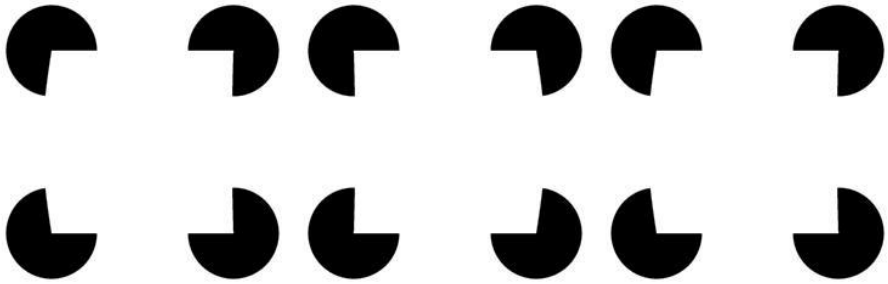

Figure 1.4. An example of crossed and uncrossed-disparity surfaces in stereoscopic Kanizsa figures. Cross fusing the left and center images produces the percept of an occluding crossed-disparity illusory surface, while fusing the center and right images produces an occluded uncrossed-disparity illusory surface.

It is well established that binocular disparity can play a significant role in the perception of illusory surfaces (Carman & Welch, 1992; Ramachandran, 1986; Vreven & Welch, 2001). Furthermore, given the sparse nature of the figures, it is not surprising that the inducer features are critical to the formation of the illusory 3D surface. Apart from Carman and Welch's (1992) qualitative assessment and Ramachandran's (1986) experiments that showed that 3D surface interpolation is involved in the perception of 3D Kanizsa figures, the underlying process that form these illusory surfaces has received little empirical attention. The experiments outlined here explored two possible approaches to 3D surface formation in illusory figures. One possibility is

that the local disparity information at the inducing elements is simply propagated via interpolation between inducers to form a coherent illusory surface. Another possibility is that the 2D illusory boundaries are first extracted and that the relative disparity between these illusory boundaries (along with the disparity of the inducers) defines the surface in depth. However, these two processes are not necessarily mutually exclusive.

1.4.1. Depth from Inducer Disparity Alone

If only the luminance-defined disparity at the inducing elements was used to define the shape of the 3D Kanizsa surface, then the disparity signal defined by the vertical inducing edges must be propagated across the region of uniform luminance via disparity interpolation. This process estimates the shape and position of regions with homogeneous luminance by assigning depth values based on the luminance-defined disparity of adjacent elements (Yang & Blake, 1995). Disparity interpolation can promote the percept of 3D illusory contours and surfaces in stimuli with very sparse texture information (Julesz, 1971; Warren, Maloney, & Landy, 2002, Wilcox, 1999), or as described above, with no texture information at all (Carman & Welch, 1992). The interpolation of disparity-defined illusory surfaces has been described as a feed-forward process with at least two stages: (i) The initiation of 3D contour formation between inducing edges from the combination of partially occluded 2D features and disparity information, (ii) the consequent interpolation of the depth signal along the illusory boundaries and the surface they define (Kellman & Shipley, 1991; Mitchison & McKee, 1987a, 1987b; Ringach & Shapley, 1996; Yang & Blake, 1995). According to this description, during modal completion of 3D Kanizsa figures, the crossed-disparity at the vertical edges of the inducers is propagated along the illusory contour between inducing elements and across the blank regions to form a 3D illusory surface. To do so depth values assigned to untextured regions are estimated from the initial

disparity signal at the inducing elements (Yang & Blake, 1995). The properties of stereoscopic surface interpolation have been extensively studied in previous psychophysical experiments (Glennerster, McKee, & Birch, 2002; Vreven & Welch, 2001; Wilcox & Duke, 2005, Yang & Blake, 1995).

1.4.2. Depth from Illusory Contour Disparity

It is also possible that the depth percept from stereoscopic Kanizsa figures is the result of the extraction of disparity from the 2D illusory boundaries formed by the inducing edges. While to date it has not be shown that the visual system extracts disparity from illusory contours, this hypothesis is consistent with increasing evidence that illusory boundaries are encoded by the human visual system in the same manner as luminance-defined contours (Larsson et al., 1999; von der Heydt et al., 1984), share similar perceptual effects (Paradiso et al., 1989; Smith & Over, 1979; Vogels & Orban, 1987; Wilcox & Duke, 2003), and exhibit rivalry with luminance-defined edges (Fahle & Palm, 1991; Harris & Gregory, 1973). While V1 has the ideal neural substrate for computing the geometry of curvilinear structures (Roelfsema et al., 1998), recent temporal studies, in conjunction with measures of neural activation, suggest that the representation of a coherent global percept may require concurrent activation in both V1 and higher-level areas (Lee & Mumford, 2003; Stanley & Rubin, 2003; VanRullen & Thorpe, 2001). To date, no direct evidence has shown that area V1 contains neurons that perform or encode contour interpolation; however, neurological studies have revealed that initial illusory contour detection in cortical area V2 is followed by latent responses in V1 and V2. These responses are thought to reflect feedback from the initial response from higher order areas that represent information the global context (Lee & Nguyen, 2001; von der Heydt et al., 1984). The potential impact of mid-level processing on activity in V1 and V2 is consistent with emergent theories and computational

models of vision that support rapid recurrent feedback (Lee & Mumford, 2003). For example, Wokke et al. (2013) recently demonstrated the existence of this rapid feedback loop between lateral occipital (LO) areas and V1/V2 using transcranial magnetic stimulation. By disrupting processing in V1/V2 and LO at different moments during a discrimination task using 2D Kanizsa figures, they revealed that the two areas are involved in an inverse hierarchical feedback loop. These studies are often used to refute evidence of a strictly feed-forward model of contour interpolation. Recurrent feedback models that support concurrent activation of high-level surface representations and early visual areas may help explain how illusory contours can be induced by partially occluded surfaces without relatable inducing edges (Anderson & Julesz, 1995; Gillam & Nakayama, 2002). In addition, recurrent feedback hypotheses provide a framework in which global contributions to surface completion can resolve the border-ownership ambiguities in illusory surfaces (Anderson, 2007; Kogo et al., 2014).

If disparity signals are extracted from 2D illusory contours, the 2D interpolation of the illusory boundaries must be completed before the disparity of the illusory surface is determined. Evidence from single-unit recordings shows that stereoscopic surface representations exist in early visual areas. For instance, neurons in areas as early as V2 can encode disparity gradients (Qiu & von der Heydt, 2005). In addition, Mendola et al. (1999) demonstrated that neurons in areas V3 and V7 respond to both illusory Kanizsa figures and stereoscopic contours defined by random dot stereograms. The critical distinction between explanations of perceived 3D illusory surfaces based solely on conventional feed-forward mechanisms and those based on recurrent hierarchical feedback is the point at which binocular disparity information contributes to the computation of the perceived depth of the surface.

1.5. Current Study

The aim of the experiments presented here is to understand the nature of the disparity signal that underlies the perception of illusory stereoscopic surfaces. To accomplish this, I separately evaluated the contribution of the conventional luminance-defined disparity of the inducers and the putative retinal disparity of the illusory boundaries. While previous studies have used 2D Kanizsa figures to investigate the spatial and temporal properties of perceived shape from illusory boundaries, they typically report subjective ratings of 'clarity' (Shipley & Kellman, 1992) or estimates of visual completion (Gold et al., 2000; Ringach & Shapley, 1996). Unlike 2D Kanizsa figures, 3D Kanizsa stimuli contain quantitative depth information via disparity. Thus, using these stimuli it is possible to assess the perceived depth of the interpolated surfaces and directly examine how this percept is influenced by properties of the inducing elements and illusory boundaries.

In the studies outlined here I systematically varied the 2D and 3D properties of stereoscopic Kanizsa configurations and assessed the impact on perceived depth. In Chapter 2, to ensure a reliable comparison between surface configurations, I determined the contrast of a stereoscopic luminance-defined surface that was approximately perceptually matched to the salience of a stereoscopic illusory surface. In Chapter 3, I varied the magnitude of disparity along the vertical inducing edge to determine the individual diplopia points for the inducing edge of the stereoscopic Kanizsa figure. Using individual interocular distances, perceptual matches, and diplopia points I created a stimulus set for each observer that consisted of a range of fused and diplopic stereoscopic surfaces in which the magnitude of disparity and the salience of the surfaces was equated. In Chapter 4, using these stimulus sets I compared the perceived depth at the peak of the illusory and luminance-defined surfaces to determine whether illusory contour interpolation follows the same trajectory as the luminance-defined template. Since the position of the peak of an illusory boundary in 3D is poorly constrained, it is possible that when illusory

contours cannot be fused, the visual system will interpolate a shallower surface curvature. If there is a significant change in the magnitude of perceived depth at the surface peak when the disparity signal at the inducers is unchanged, then disparity interpolation plays a key role in determining surface shape. Lastly, in Chapter 5, I determined if the variability of perceived depth between stimulus conditions was due to the precision of the disparity signal along the vertical surface edge. To assess this, I measured the precision of perceived depth estimates and determined if the disparity at the inducing element was sufficient to support accurate interpretation of the depth of the interpolated surface. Ultimately this work provides important insight into binocular disparity processing, and how 2D and 3D information is combined to generate stable percepts of surfaces in ambiguous or ill-defined stimuli. If illusory boundaries provide additional disparity information for binocular correspondence then the contours must be established prior to disparity estimation, likely reflecting concurrent feedback between early and late visual areas.

1.6. General Methods

1.6.1. Observers

Seven observers (including the author) were recruited. The stereoacuity of each observer was assessed using the Randot^{TM} stereoacuity test to ensure that observers could detect depth from binocular disparities of at least 40 seconds of arc. All observers had normal or corrected-to-normal vision. The average interocular distance of the observers was 60mm with a range of 58mm to 62mm. These same observers participated in all subsequent experiments. The research protocol used here and in all subsequent experiments was approved by the York University research ethics board and adheres to the tenets of the Declaration of Helsinki.

1.6.2. Stimuli

All Kanizsa figures were generated using OpenGL 3D graphics within the Psychtoolbox package for MATLAB on a Mac OS X computer (Brainard, 1997; Pelli, 1997). The figures were rendered as 3D objects in OpenGL using perspective projection with an asymmetric frustum configuration. Using perspective projection minimizes the conflict between perspective and binocular disparity by ensuring that the projection of the stimulus in each eye's view is consistent with the curvature defined by disparity. Each 3D rendered Kanizsa figure was created by drawing four fronto-parallel black circles (0.81 cd/m^2) with a grey occluding curved surface template with the same luminance as the background (50.3 cd/m^2). The curvature of the luminance template was defined as a sine wave with an amplitude calculated from the disparity at the peak along with the interocular distance of the observer using a conventional formula, which relates disparity to predicted depth at a known viewing distance (see Howard & Rogers, 2012, pp. 152-154).

In a series of preliminary studies, I evaluated the perceived depth of stereoscopic illusory Kanizsa figures with crossed and uncrossed disparities at the vertical inducing edge. Regardless of the direction of disparity at the inducing edge, each monocular illusory Kanizsa surface is seen to lie in front of the inducing elements. As discussed in Section 1.4, when the illusory surface extends behind the inducing elements (uncrossed disparity) there is conflict between the disparity signal and the 2D monocular depth order information. Results of a preliminary study confirmed that this conflict degrades the perceived depth at the peak of the surface. In order to avoid the effects of cue conflict, I ensured that the direction of binocular disparity was always consistent with the 2D occlusion geometry by rendering images with crossed disparity only (Gregory & Harris, 1974; Lawson et al., 1974).

In all stimuli, the diameter of the inducers was 0.8deg and the distance between the centers of adjacent inducers was 1.7deg. According to these dimensions, the support ratio for each monocular Kanizsa figure was 0.5 when the disparity at the peak was zero; where support

ratio is defined as the ratio of the length of luminance-defined edge to the total edge length (Shipley & Kellman, 1992). To equate the disparity for all observers, the lateral separation of the two frustums at the virtual screen was equivalent to the observer's interocular distance. Each monocular image was exported as a MATLAB mat-file, which contained the raw image matrix for each disparity-defined Kanizsa figure. The geometry of OpenGL's projection matrix was designed to replicate the viewing geometry within our modified Wheatstone mirror stereoscope. The configuration of the projection matrix ensured the two frustums converged at a distance equivalent to the screen plane.

1.6.3. Apparatus

Stimuli were presented using the Psychtoolbox package (Brainard, 1997; Pelli, 1997) for MATLAB on a Mac OS X computer. All stimuli were presented on a modified Wheatstone mirror stereoscope consisting of two LCD monitors (Dell U2412M) with a viewing distance of 74cm and a fixed chin rest to maintain stable head position during testing. The monitor resolution was 1920 x 1200 pixels with a refresh rate of 75Hz. At this resolution and viewing distance, each pixel subtended 1.26 min of visual angle. Observer's interocular distance was measured using a Richter digital pupil distance meter™. All testing took place in a darkened room except for the light from the stereoscopic display. All subsequent experiments used the same stereoscopic apparatus.

Chapter 2

Lightness

2.1 Perceived Lightness of Illusory Boundaries

The perception of lightness is closely related to perceived depth (Gilchrist, 1977; Gilchrist, 1980). In the case of illusory boundaries, depth order can directly affect the perception of photometric properties and vice versa (Adelson, 1993; Knill & Kersten, 1991; Wishart, Frisby, & Buckley, 1997). Thus, prior to comparing the impact of luminance-defined and illusory contours on perceived depth it is important to equate the perceived lightness of the two types of surfaces. Early studies of illusory contour perception used a range of psychophysical methods to quantify perceived lightness. For instance, investigators have used rating scales (Jory & Day, 1979), magnitude estimation (Halpern, 1981; Petry, Harbeck, Conway, & Levey, 1983) and matching tasks (Brussel, Stober, & Bodinger, 1977; Spillman, Fuld, & Neumeyer, 1984) to match the perceived lightness of illusory figures to a luminance-defined standard. Despite differences in procedures and stimuli, brightness matches appear consistent across studies (Dresp, 1992; Spillman et al. 1984).

In a preliminary experiment I asked each observer to match the salience of a luminance-defined surface to the perceived brightness of an illusory surface. Initially I used a 2-down 1-up staircase procedure (Levitt, 1970), in which observers matched the luminance of a 2D luminance-defined surface to the perceived brightness of a 2D illusory Kanizsa square (Figure 2.1). On each trial, the two surfaces were presented simultaneously for 320ms (the same exposure duration used in all subsequent depth estimation experiments). The contrast of the 2D luminance-defined surface was varied from trial-to-trial and observers were asked to indicate which of the two surfaces appeared brighter. The mean of all observers' perceived brightness matches (n=7) were 51.9 cd/m^2 (SD=1.0 cd/m^2) with a range from 50.9 to 53.5 cd/m^2. These values represent the luminance of a 2D surface that has the same perceived brightness as an illusory surface (with the same spatial dimensions). The mean contrast of the brightness matches (1.7%) was consistent with previously reported contrast thresholds for the detection of illusory contours in 2D Kanizsa

figures that report detection thresholds as low as 1% to 3% (Li & Guo, 1995). Observers were able to make these brightness matches consistently; however, when the luminance levels obtained from this matching task were used to define a stereoscopic surface, observers reported that they had difficulties perceiving the surface.

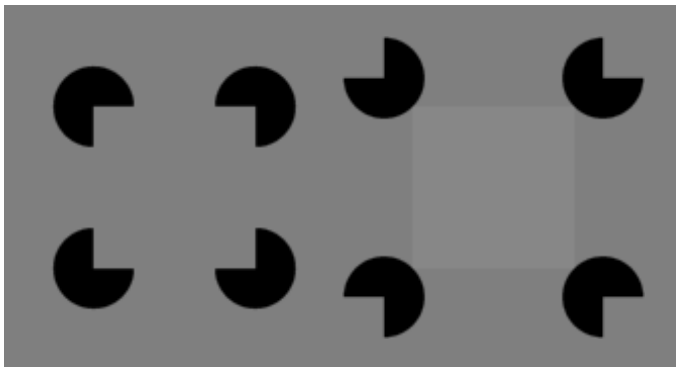

Figure 2.1. An illustration of the stimuli used in the 2D staircase procedure. The illusory Kanizsa figure is shown on the left and the luminance-defined surface with rotated inducing elements is shown on the right.

The effect of luminance contrast on stereoscopic thresholds is well established (Frisby & Mayhew, 1978; Legge & Gu, 1989; Ogle & Weil, 1958). Legge and Gu (1989) demonstrated that the stereoscopic threshold is approximately inversely related to the square root of the Michelson contrast, at contrasts ranging from 0.01 to 1.0. Closer examination of the perceptual matches from the preceding 2D brightness match revealed that they fall within this critical contrast range with a mean Michelson contrast of 0.02. At this low contrast, it has been shown that luminance values are close to the threshold contrast for disparity detection, which introduces considerable noise in both discrimination and magnitude estimation (Howard & Rogers, 2012). To avoid this issue, I equated the illusory and luminance-defined surfaces using a novel suprathreshold task described below.

2.1.1 Rationale

In the pilot experiment described above, some observers reported that perceived depth of the luminance-defined surfaces increased as the surface luminance increased. Previous studies that examined the relationship between contrast and perceived depth showed that lowering the contrast of a stimulus at a fixed disparity caused it to appear more distant (Fry, Bridgman, & Ellerbrock, 1949; Rohaly & Wilson, 1999; Schor & Howarth, 1986). In addition, the magnitude of perceived depth from disparity can directly depend on the luminance contrast of the surface (Chen, Chen, & Tyler, 2016). I capitalized on this by creating a two interval forced choice (2IFC) brightness-matching paradigm in which observers compared the perceived depth of an illusory stereoscopic surface and a luminance-defined surface with equivalent relative disparity along the inducing edge. By varying the luminance of the luminance-defined surface, I determined the approximate luminance value at which the perceived depths of the illusory and luminance-defined peaks were equivalent. I used this matched luminance value in subsequent comparisons of illusory and luminance-defined surfaces.

2.2. Methods for Experiment 2.1.

Observers

See Section 1.6.1.

Stimuli

The stimuli consisted of stereoscopic illusory Kanizsa figures and luminance-defined comparison patterns with rotated inducing elements. All stimuli were generated as described in Section 1.6.2. The test figures were presented at the center of the display on a grey background (50.3 cd/m^2). Above and below the central (5.2 x 10.5deg) region an array of high contrast (65.6 cd/m^2) circles (radius = 0.21deg) were positioned on the fixation plane at a standing disparity of

0.42deg. The pattern of circles was randomized from trial to trial so they provided no consistent position cue, but on each trial they provided a strong fusion lock, and reference plane.

The two stimulus configurations (illusory and luminance-defined) were presented sequentially in a 2IFC paradigm (see Figure 2.2). The illusory Kanizsa figure was always presented in the first interval with a fixed crossed disparity of 0.13deg (between the fixation plane and the illusory peak defined by the template). In the second interval, a luminance-defined figure with rotated inducing elements was presented with one of nine grey levels (luminance ranged from 52.3 to 55.3 cd/m^2). The luminance-defined surface had the same dimensions and relative disparity as the template used to create the illusory Kanizsa figure. To keep the stereoscopic information and configuration as consistent as possible (see Figure 2.1) the inducers were present, but rotated 180 degrees so they created no illusory surface. They were shifted diagonally outwards by 1.2deg, so they abutted the corners of the luminance-defined surface and had zero disparity relative to the fixation plane.

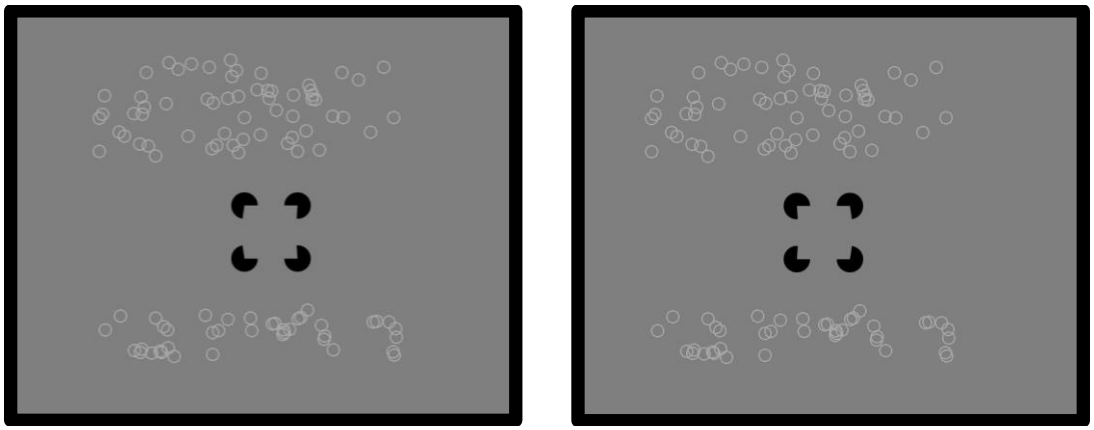

Figure 2.2. An illustration of the stimulus configuration used in the 2IFC brightness-matching task. An array of circles served as the fusion field at the top and bottom of the screen that formed the fixation plane. The fixation plane was displayed at a fixed uncrossed disparity relative to the screen plane. The stimulus was presented at the center of the screen, such that the relative disparity of the inducing elements equaled the disparity of the fixation plane.

Apparatus

The apparatus was the same as described in Section 1.6.3.

Procedure

Observers were asked to indicate whether the luminance-defined surface had more or less depth than the illusory reference figure. On each trial they initially fixated a Nonius cross positioned at the center of the screen and aligned the vertical contours of the cross to fixate on the zero disparity plane (Howard & Rogers, 2012). Once the Nonius lines were aligned observers pressed a gamepad button to display the illusory Kanizsa reference stimulus for 320ms. This was followed by the luminance-defined surface at one of nine randomly selected luminance values for 320ms. The latency to initiate a vergence eye movement ranges from about 160 to 200ms depending on the stimulus configuration (Tulunay-Keesey & Jones, 1976; Westheimer & Mitchell, 1969; Yang, Bucci, & Kapoula, 2002), while the total time to complete a vergence eye movement is 800ms (Rashbass & Westheimer, 1961). A duration of 320ms ensured that there was sufficient time for the illusory surface to form (approximately 140 to 200ms, see Kogo, Liinasuo, & Rovamo, 1993; Reynolds, 1981; Ringach & Shapley, 1996) while restricting the amount of time observers had to complete a vergence eye movement. After viewing the illusory reference and luminance-defined comparison, observers pressed one of two gamepad buttons to indicate whether the stimulus in the second interval had more or less depth relative to the first interval. Each luminance value was randomly presented 30 times, for a total of 270 trials. Prior to the test session, observers completed a brief practice session consisting of 27 trials to familiarize themselves with the task.

2.3 Results and Discussion

A cumulative Gaussian was used to fit the psychometric data and compute the point of subjective equality (PSE) for each observer (Figure 2.3). The analysis was performed in R using

the glm() function in the "stats" package and the error of the estimate was determined using bootstrapped confidence intervals calculated using Monte Carlo simulation methods run 1,000 times for each dataset (Wichmann & Hill, 2001a, 2001b). The average PSE across observers was 53.7 cd/m^2 (95% CI: 53.5, 53.8) with a range from 53.4 to 54 cd/m^2.

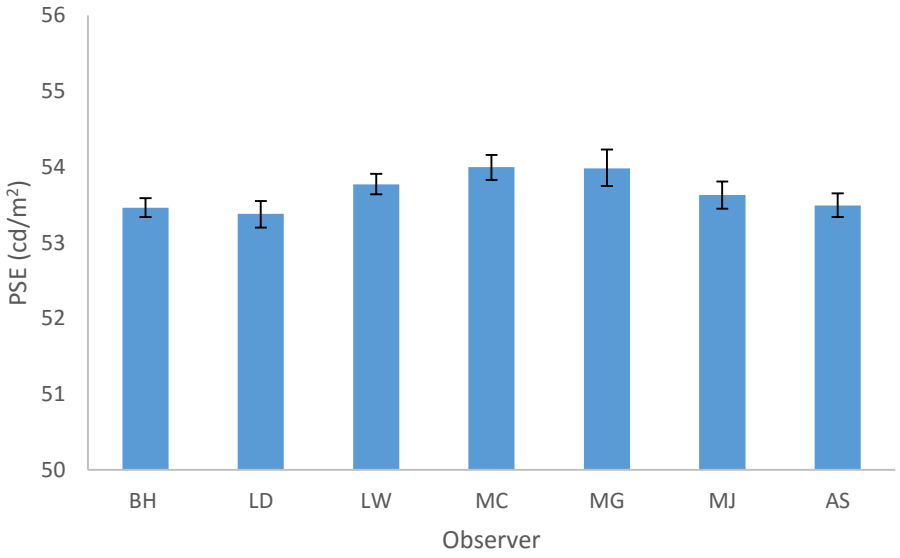

Figure 2.3. Bars represent individual PSEs. Error bars represent bootstrapped 95% confidence intervals.

The PSE for each observer is plotted in Figure 2.3. The luminance value represents the brightness of a stereoscopic luminance-defined surface that had the same perceived depth as a stereoscopic illusory surface with equivalent disparity information along the inducers. These values were used in subsequent experiments for each observer when luminance-defined surfaces were compared with illusory surfaces. Unlike the estimates obtained in the initial study, when these matched luminance values were used to generate curved stereoscopic surfaces they produced a stable 3D surface that appeared perceptually equivalent to the 3D illusory surface.

Chapter 3

Inducer Diplopia

3.1 Introduction

In Chapter 4 I assessed the perceived depth in 3D Kanizsa figures when the inducer disparity was reliable and when it was degraded. To degrade the disparity signal without changing other stimulus details that might have influenced perception of the illusory surface, I simply presented the same stimuli at an inducer disparity that was difficult to fuse. Within Panum's fusional area disparate stimuli appear fused and quantitative depth percepts are obtained (Howard, 1995; Ogle, 1964). At larger disparities, there is a point at which fusion is lost: the diplopia threshold. At this point observers are able to make quantitative depth estimates, but with less precision (Ogle, 1964). By systematically varying the relative disparity of the inducing edges I calculated the point at which observers no longer perceieved a perceputally fused luminance edge. A range of test stimuli were created by varying the amplitude of the sinusoidal surface to cover a range of disparities that spanned the diplopia threshold for each observer. Diplopia thresholds vary from person to person, so the diplopia point was determined for each observer.

3.1.1 Rationale

The purpose of the experiment outlined below was to measure individual diplopia thresholds for the vertical inducing edges of the Kanizsa figure shown in Figure 3.1. I varied the relative disparity of the inducing edge using a method of constant stimuli and calculated the disparity at the tip of the inducing edge when observers reported that the inducers were no longer fused. In Chapter 4, I used the diplopia thresholds to select the range of test disparities for each observer.

3.2 Methods for Experiment 3.1

Observers

The observers that participated in this experiment also took part in Experiment 2.1.

Stimuli

Stimuli consisted of 3D illusory Kanizsa figures with the same array of high contrast circles used in Experiment 2.1 (see Figure 3.1). The relative disparity along the inducing edge increased from the corner of the occluding surface to the tip of the vertical inducing edge; I defined inducer disparity as the disparity between the tips of the vertical inducer edges. The stereoscopic Kanizsa figures were presented with one of eight crossed inducer disparities (0.06, 0.09, 0.11, 0.14, 0.17, 0.20, 0.22, 0.25deg) for 200ms. An exposure duration of 200ms prevented the observer from completing a vergence eye movement while the stimulus was presented (Westheimer & Mitchell, 1969). The combination of the dichoptic Nonius cross, fusion field, and brief exposure duration helped observers maintain fixation on the depth plane containing the inducing elements while they performed the task.

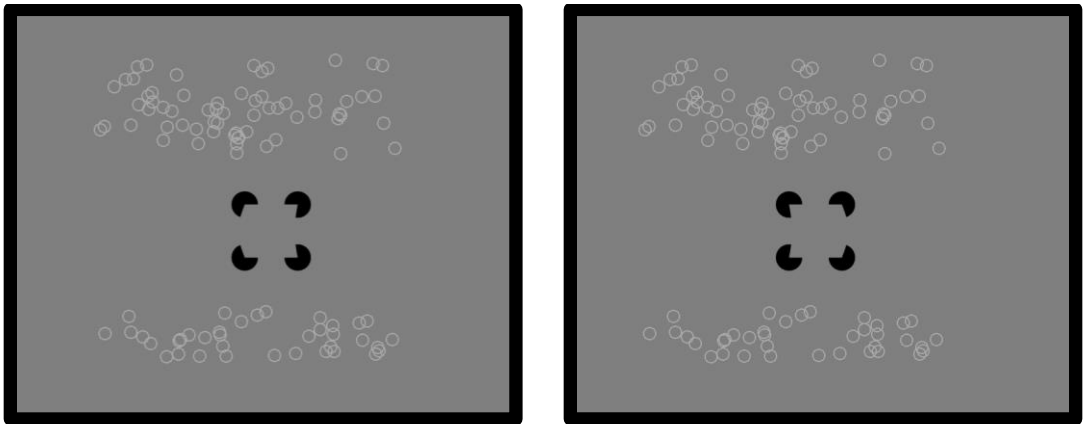

Figure 3.1. An illustration of the stimulus configuration used in the inducer diplopia task. An array of circles served as the fusion field at the top and bottom of the screen forming the fixation plane. The illusory Kanizsa figure was presented at the center of the screen, such that the relative disparity of the outer edge of the inducing elements equaled the disparity of the fixation plane. Note that the inducing edges in the example above are not perceptually fused when converged on the fixation plane.

Apparatus

The apparatus was the same as described in Section 1.6.3.

Procedure

Diplopia thresholds were measured using a single alternative forced-choice (AFC) paradigm and the method of constant stimuli. Observers fixated on a Nonius cross at the center of the screen and, once the Nonius cross was aligned, they pressed a button to display the illusory Kanizsa figure for 200ms. On each trial, observers judged whether the curved vertical edge of the inducing element appeared single or double using the gamepad. Test disparities were randomly presented 30 times apiece, for a total of 240 trials. Prior to the test session, observers completed a brief practice session consisting of 24 trials to familiarize themselves with the stimuli and task.

3.3 Results and Discussion

The proportion of "double" responses as a function of inducer disparity was plotted for each observer (Figure 3.2). A cumulative Gaussian was used to fit this psychometric data and the

diplopia threshold was calculated as the 50% point on the psychometric function. The analysis was performed in R using the glm() function in the R "stats" package. The error of the estimate was determined using bootstrapped confidence intervals calculated using Monte Carlo simulation methods run 1,000 times for each dataset (Wichmann & Hill, 2001a, 2001b).

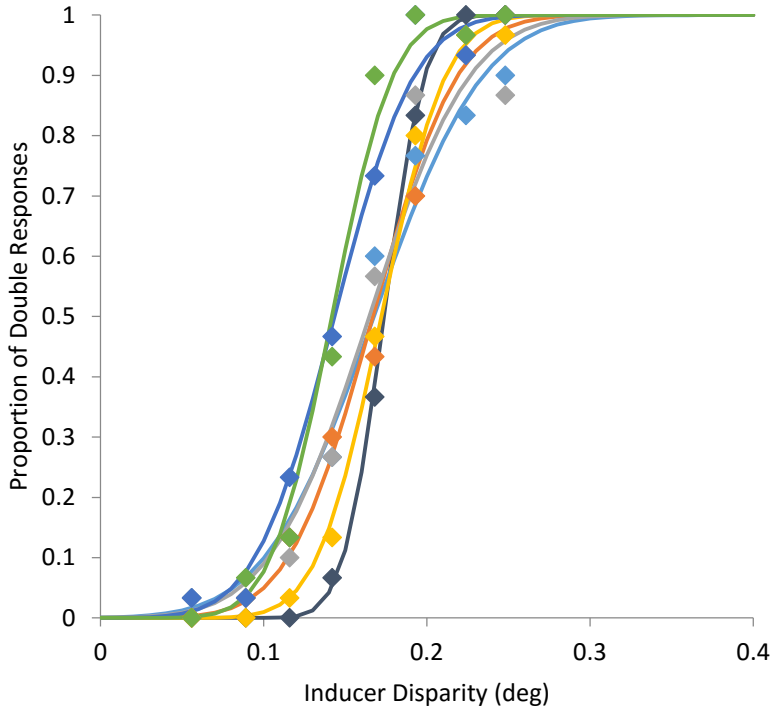

Figure 3.2. The fitted psychometric function (cumulative Gaussian) for each observer's dataset (n=7). The PSE for each function represents the relative disparity between the tips of the vertical inducing edge at the diplopia threshold.

After a brief practice session, all observers easily identified whether the vertical inducing edge was perceptually diplopic or fused. The diplopia points ranged from 0.14 to 0.17deg with an average of 0.16deg (95% CI: 0.15 0.17). Five of the seven observers were at the upper end of this range between 0.16 and 0.17deg, while the remaining two observers' thresholds were approximately 0.14deg. The diplopia point calculated for each observer (see Appendix A) was used in subsequent experiments for comparison with performance when the inducers were fused.

Chapter 4

Accuracy

4.1 Introduction

A variety of psychophysical paradigms have been used to quantify the perceived shape of 2D Kanizsa figures. For example, investigators have reported subjective ratings of 'clarity' (Shipley & Kellman, 1992), estimates of visual completion (Gold et al., 2000; Ringach & Shapley, 1996), or orientation (Westheimer & Li, 1997). While these studies provide valuable information about the properties of inducing elements that dictate the perceived salienceand position of 2D illusory contours, to quantify the perceived depth from disparity in stereoscopic Kanizsa figures one must use a methodology that can be used to quantify the perceived depth at a given location along the surface (e.g. the peak).

Few studies have examined the properties of disparity-defined illusory boundaries generated in Kanizsa configurations. One notable series of experiments is Ramachandran's (1986) assessment of the foreground and background segmentation in 3D Kanizsa figures. He presented a frontoparallel occluding surface defined by binocular disparity in front of a variety of background textures. His results demonstrate that planar stereoscopic illusory surfaces can capture textured background elements, which have ambiguous disparity, while similar disparity-defined surfaces without illusory boundaries do not. This is a critical distinction. Stereoscopic capture tends to occur when contour elements appear to be occluded by the foreground pattern; disparity alone creates little, if any stereoscopic capture (Howard & Rogers, 2012). The presence of an illusory surface appears to be a necessary prerequisite for stereoscopic capture in these configurations. These experiments suggest that binocular disparity *in conjunction* with occlusion relationships at inducing elements plays a critical role in establishing 3D illusory surface shape

and the interpretation of the 2D geometry of background elements. In a subsequent study Hakkinen et al. (1998) expanded Ramachandran's research to include curved and slanted illusory boundaries, demonstrating that non-planar illusory surfaces can facilitate stereoscopic capture if the period of the background texture is consistent with the 3D geometry defined by binocular disparity. Hakkinen's results were consistent with those of Ramachandran, and emphasize the combined role of occlusion geometry and the disparity signal in the creation of a coherent 3D percept.

It has been established that the introduction of even small disparity differences between the inducing edges produces striking changes in the perceived shape of 3D curvilinear illusory surfaces (Carman & Welch, 1992). As discussed in Section 1.4, the disparity signal at the inducing edge determines the structure of the 3D illusory surface via disparity interpolation, whereby the unambiguous disparity signal at the vertical inducing edge is propagated along the vertical illusory contours between adjacent elements to form a complete surface. Despite the large ambiguous central region in Kanizsa configurations, the perceived shapes of these stereoscopic illusory surfaces demonstrate remarkable shape invariance and view stability (Carman & Welch, 1992). However, studies of disparity-based surface interpolation largely focus on the interpolation of sparse disparity-defined elements along surface edges (Mitchison & McKee, 1985; Yang & Blake, 1995); little empirical attention has been paid to how disparity interpolation propagates from a luminance edge to an illusory surface. The goal of this chapter was to evaluate how manipulation of the disparity signal at the inducing edge affects the perceived depth of the surface. To accomplish this, I used a depth magnitude estimation paradigm that allows observers to estimate the depth at the 3D surface peak as described below.

4.1.1 Depth Magnitude Rationale

A depth magnitude estimation paradigm was used to assess the perceived depth at the surface peak of illusory and luminance-defined surfaces at a large range of fused and diplopic inducer disparities. The aim of this experiment was to better understand the nature of interpolation of the disparity signal in these illusory surfaces. To do this, I measured the perceived depth magnitude at the surface peak, when the inducer edges were fused and when the disparity signal at the inducers was less reliable (at the diplopia point). Further, the comparison of the magnitude of perceived depth between illusory and luminance-defined surfaces reveals whether the trajectory of interpolation in the illusory surface differs from the sinusoidal curvature of the luminance-defined template. If there is a difference in the magnitude of perceived depth between the surface peaks when the disparity within the inducing region is equivalent, then disparity interpolation plays a key role in determining illusory surface shape. In addition, if there is a larger difference in the perceived location of peaks between the illusory and luminance-defined surfaces beyond the diplopic threshold compared to the fused range, then the visual system interpolates the illusory boundary to a shallower surface when the disparity along the inducing edge is less reliable.

4.2 Methods for Experiment 4.1

Observers

The observers that participated in this experiment are described in Section 1.6.1.

Stimuli

Three stimulus conditions, (i) Illusory Only, (ii) Low Contrast, and (iii) Combined, were created using the individual perceptual matches and diplopia points calculated for each observer in Experiments 2.1 and 3.1. The Illusory Only condition consisted of a stereoscopic Kanizsa figure in which only illusory contours defined the position of the surface peak. The Low Contrast

condition consisted of a luminance-defined stereoscopic surface with rotated inducing elements (see Experiment 2.1). The luminance of the central region was set to the perceptual match calculated for each observer in Experiment 2.1. Lastly, the Combined condition consisted of a stereoscopic Kanizsa figure with the perceptually matched luminance-defined surface in the central region. In this case, all the supporting geometry for illusory contour generation was present, but the surface was also defined by explicit luminance edges. Examples of each of these stimulus configurations and the features that define the shape of the surfaces can be seen in Figure 4.1. All stimuli were generated as described in Section 1.6.2. The stimulus arrangement was the same as that shown in Figure 3.1 with an upper and lower array of circles to aid fusion. Each figure was presented with one of eleven crossed inducer disparities (0, 0.03, 0.06, 0.09, 0.12, 0.14, 0.17, 0.20, 0.22, 0.25, and 0.27deg).

Table 4.1

Stimuli for Depth Magnitude Task

Stimulus Condition	Surface Features	Stereopair
Illusory Only	• Occlusion features • Disparity signal at the inducing edge	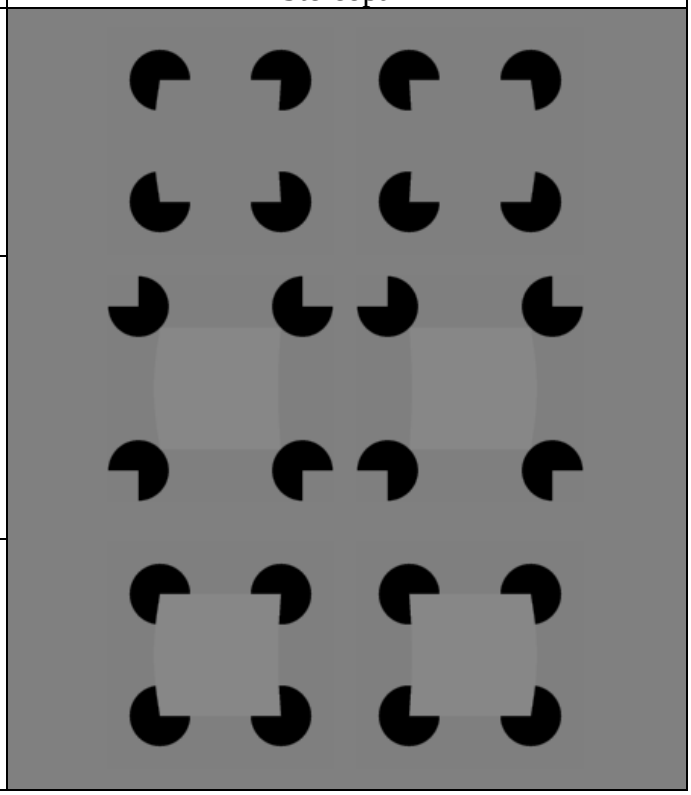
Low Contrast	• Disparity signal at low contrast surface edge	
Combined	• Occlusion features • Disparity signal at the high contrast inducing edge and low contrast surface edge	

Note. The stereopairs are arranged for crossed fusion.

Apparatus

Stimuli were viewed stereoscopically using the apparatus described previously (Section 1.6.3). Depth estimates were recorded using a purpose-built touch sensitive sensor. A rectilinear SoftPot membrane potentiometer (SpectraSymbol) was mounted on a thin aluminum bar. The sensor strip was 200mm long and 7mm wide with a resistance of 10 kOhm. The potentiometer allowed linear measurements along the 200mm length, with a resolution of approximately 0.2mm. Responses were read using an analog to digital converter and a 160bit micro controller. Prior to testing observers rested their thumb against a rod at one end of the haptic sensor strip, and the rod was adjusted so the end of the sensor strip was aligned to the outer edge of the observer's thumb (this compensated for differences in thumb width). During testing observers

pressed their index finger along the length of the sensor strip to indicate the magnitude of their depth estimate. A small red LED positioned in front of the stereoscopic mirrors, 10.8deg below the line of sight to the stimulus, illuminated when sufficient pressure was applied to the sensor strip. Observers were free to adjust their fingers until they were satisfied with their response and pressed the space bar on the computer keyboard to initiate the next trial. The recorded voltage was converted into millimetres using a MATLAB script. Between trials observers were asked to reposition their index finger to the base of the sensor, and to refrain from looking down at their hand while making their depth estimates.

Procedure

On all trials, observers were asked to indicate the amount of depth they perceived between the fixation plane containing the inducing elements and the peak of the curved surface. The stimulus configuration and presentation protocol was the same in all conditions. Observers began by fixating on a Nonius fixation cross. When they perceived the cross as aligned, they pressed a gamepad button to display the stimulus for 320ms. The three stimulus configurations were assessed in separate blocks and in each block eleven test disparities were randomly presented 12 apiece, for a total of 132 trials per condition. The test order was randomized across observers and between each block of trials observers received a short break. Prior to each test session, observers completed a brief practice session consisting of 33 trials to familiarize themselves with each of the stimulus conditions and apparatus.

4.3 Results and Discussion

Figure 4.1 shows the mean estimated depth for each of the three stimulus configurations plotted as a function of the relative inducer disparity in degrees. A repeated-measures analysis of variance was used to examine the differences in perceived depth for the three stimulus conditions

in the fused and diplopic ranges. From Figure 4.1, it is clear that the variance of observer's perceived depth estimates increases as a function of inducer disparity. This is not surprising given that discrimination thresholds have been shown to increase as a function of disparity (Blakemore, 1970; McKee, Levi, & Bowne, 1990). A Levene's test on the standardized residuals confirmed that the variance is indeed heterogeneous ($p=0.02$), which violates the assumption of homoscedastic variance. To avoid this violation a separate analysis of variance was performed for the fused and diplopic ranges (Levene's test $p>0.05$). In the fused range test disparities were 0.03, 0.06, 0.09, 0.11, and 0.14deg, while in the diplopic range they were 0.17, 0.20, 0.22, 0.25, and 0.27deg. In the fused range the analysis revealed an expected significant effect of Inducer Disparity, $F(1.2,7.2)=46.44$, $p<0.0001$; $\eta^2=0.58$, but no significant effect of Stimulus Condition, $F(2,12)=0.65$, $p=0.54$; $\eta^2=0.01$, or interaction between the two variables, $F(3.7,22.5)=2.05$, $p=0.13$; $\eta^2=0.02$. Similarly, in the diplopic range there was a highly significant effect of Inducer Disparity, $F(4,24)=34.72$, $p<0.0001$; $\eta^2=0.22$, a lack of significant difference between Stimulus Conditions, $F(2,12)=2.32$, $p=0.14$, $\eta^2= 0.03$, and no significant difference between stimulus conditions as a function of Inducer Disparity, $F(8,48)=0.20$, $p=0.99$, $\eta^2=0.001$.

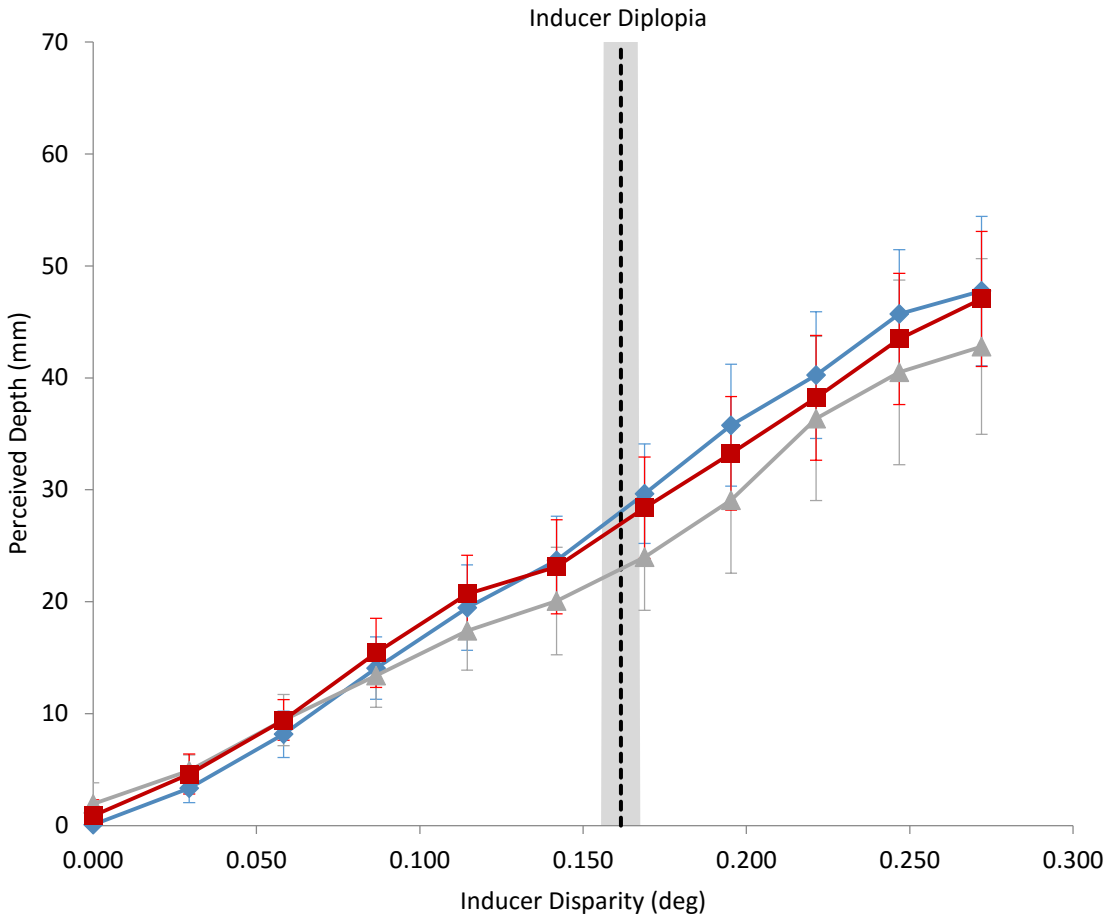

Figure 4.1. Mean depth estimates (n=7) for each of the three stimulus conditions: Illusory Only (diamonds), Low Contrast (triangles), and Combined (squares). The black dotted line represents the mean inducer diplopia point (obtained in Experiment 3.1) and the shaded region represents one standard error of that estimate. Error bars represent one standard error of the mean.

Analyses of the fused and diplopic data show that there was no difference in the perceived depth between the Illusory, Low Contrast, and Combined conditions. This result was surprising given the differences between these stimuli, and the information used to define the peak of the surfaces in each condition. However, as noted above, the variance of observers' estimates increased as a function of inducer disparity, becoming quite large when the inducing edge was perceptually diplopic, suggesting that there might be large interobserver differences in perceived depth at these disparities. Inspection of the individual depth estimates confirmed this observation. In addition, some observers demonstrated differences between the Illusory, Low Contrast, and

Combined stimulus conditions, while other observers demonstrated little difference in perceived depth. It is possible that this disparity-dependent variability may have obscured differences between the surface conditions.

Another interesting aspect of the results shown in Figure 4.1 was that none of the three stimulus conditions showed any reduction in the perceived depth of the peak once the disparity of the inducing edge was increased beyond the diplopia point. It is well established that depth percepts can be obtained from both fused and diplopic stimuli (Blakemore 1970; Foley, Applebaum, & Richards, 1975; Ogle, 1952), but there is a point at which this is no longer true and observers begin to lose the ability to make quantitative depth estimates. Described by Ogle (1952) as the qualitative range, at these very large diplopic disparities observers are only able to judge the sign of depth. As disparity continues to increase, eventually depth percepts will be lost entirely at the upper disparity limit. However, despite the large disparity at the inducing edge the perceived depth continued to increase as a function of inducer disparity. It is possible that observers may have based their judgements on another criterion other than the depth from binocular disparity in the diplopic range. One important consideration when measuring the depth when stimuli are fully diplopic is that observers can perceive the lateral separation of the monocular images. It is possible that, even though observers are trying to report depth from disparity, their estimates are influenced by the increasing separation of the monocular features. The elimination of this information can be difficult given that the separation information is fully confounded with the binocular disparity signal (Ogle, 1953). I believe this is not a likely explanation for my results because one would expect a transition (i.e. abrupt change in the slope) in the diplopic range when observers switched to using the separation information. Instead, it is clear that the functions shown in Figure 4.1 increase smoothly across the test range.

In a follow-up study I re-examined the relationship between disparity and perceived depth for these surface configurations. I used a single AFC method that required that observers discriminate the depth between two disparity-defined objects. N-alternative forced choice methods tend to produce less variable results than magnitude estimates, and could reveal significant differences between surface conditions that were not evident in the preceding study. In our AFC task, observers used a disparity probe to indicate the perceived depth at the peak of the surface.

4.3.1 Disparity Probe Rationale

In this probe task, observers made a depth discrimination judgement between a small dark grey disk and the peak of the stereoscopic surface, which reduced the usefulness of the separation information. Disparity probes tend to provide very precise results because observers have a direct comparison and are able to rely on disparity matching, which is less variable both within and between observers than depth magnitude estimation. When using disparity probes it is important to ensure that the probe does not interfere with, or influence, the test stimulus. I anticipated that by reducing interobserver variability and the potential influence of separation information, this experiment was more sensitive to differences between the perceived locations of the peaks of the surfaces across conditions.

4.4 Methods for Experiment 4.2

Observers

The observers that participated in this experiment are described in Section 1.6.1.

Stimuli

The three surface conditions described in Section 4.2.2 were also used here. In addition, I included a fourth, High Contrast condition in which the surface boundaries are clearly visible. This stimulus consisted of a black luminance-defined stereoscopic surface (0.81 cd/m^2) with rotated inducing elements (see Section 2.2.2). In this condition the luminance-defined surface was salient, with high contrast vertical edges, thus performance should be at its best. Examples of the four conditions can be seen in Figure 4.2. As in the previous experiment, I evaluated both fused and diplopic conditions. In this study the fused standard had a fixed disparity that was well within the fused range for all observers (0.09deg). For the diplopic standard, the reference was assigned the disparity equivalent to the diplopia point for each observer (Chapter 2). A disparity probe (luminance of 22.6cd/m^2) with a diameter of 0.25deg was presented 2.1deg to the left of the center of the screen. This offset was shown in preliminary trials to minimize the influence of the probe on the interpolation of the surface. The probe was presented at one of nine crossed disparities with a unique step size for each observer. In the fused condition, the disparity values for the probe ranged from 0.06 to 0.17deg. In the diplopia conditions the disparity values of the probe ranged from 0.13 to 0.29deg. The step size was determined for each observer for each condition in a short pre-test with 5 trials per disparity level.

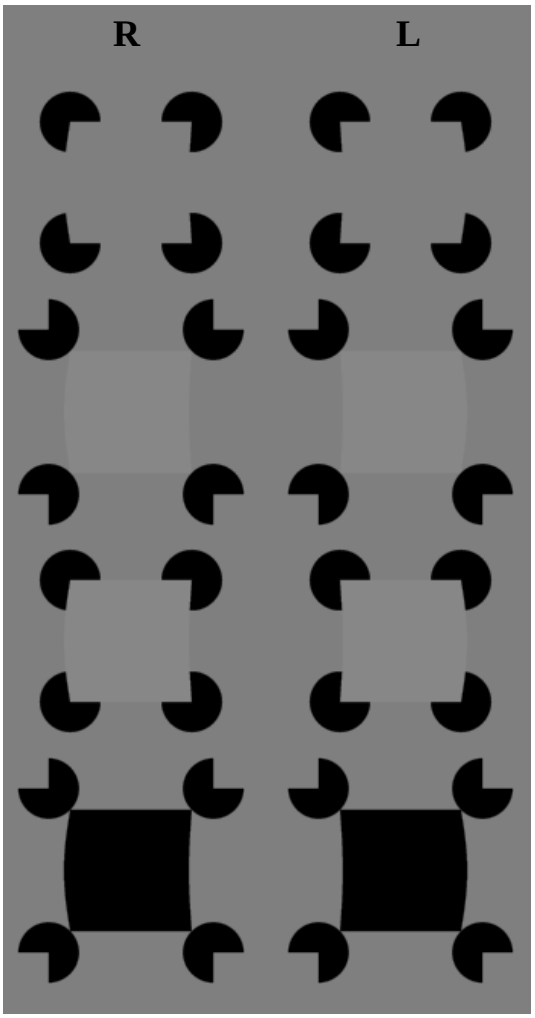

Figure 4.2. An example of the stereopairs used to generate stereoscopic surfaces for each stimulus condition (arranged for crossed fusion). From top to bottom the stimulus conditions are Illusory Only, Low Contrast, Combined, and High Contrast.

Apparatus

The apparatus was the same as described in Section 1.6.3.

Procedure

The PSE for each stimulus was measured using a 1AFC paradigm. The duration of each interval was 320ms and the four stimulus conditions were assessed in separate blocks. The disparity probe was presented at each of the nine disparity levels in random order 30 times apiece, for a total of 270 trials per condition. Each observer completed the four conditions using

the fused and diplopic standards for a total of 8 test conditions. The test order was randomized across observers and between each block of trials observers had a short break. On all trials observers were asked to indicate whether the disparity probe was positioned in front of or behind the peak of the surface. Observers press one of two possible gamepad buttons to make their response. Prior to each test session observers performed a brief practice session that consisted of 5 trials for each test disparity to familiarize them with the task and to set the appropriate step size.

4.5 Results and Discussion

The psychometric data obtained from each observer for each test condition was fit using a cumulative Gaussian. The PSE was computed for each condition at both the fused and diplopic standards for all observers (n=7). One observer was removed from the final data analysis due to an incomplete dataset, resulting in a total of six observers. The analysis was performed in R using the glm() function in the R stats package. Bootstrapped confidence intervals were calculated using Monte Carlo simulations methods run 1,000 times for each dataset (Wichmann & Hill, 2001a, 2001b).

To assess the differences in the perceived peak disparity in the four stimulus conditions a repeated-measures analysis of variance was used to compare the effect of Stimulus Configuration and Disparity Range on PSE. Disparity Range was a categorical variable that compared the mean PSE at the diplopia threshold to the fused standard. The analysis revealed a significant interaction between Stimulus Configuration and Disparity Range, $F(3,15)=33.33$, $p<0.0001$, $\eta^2=0.18$. This indicated that there was a significant difference in the disparity of the perceived peaks in the four surface conditions that differed between the fused and diplopia standards. To examine the differences in the disparity of the perceived peaks between our stimulus conditions I used

pairwise t-tests and Benjamini and Hochberg's (1995) method for controlling false discovery rates. The differences in the stimulus conditions as a function of the type of reference (fused or diplopia) are discussed below.

4.5.1 Fused Standard

The mean estimated peak disparity for the four test conditions for the fused standard can be seen in Figure 4.3 (individual psychometric functions are in Appendix B). For all observers the estimated disparity of the High and Low Contrast peaks was similar, while estimates of the Illusory Only and Combined surface peaks were shifted downwards. The pairwise t-tests confirm that all comparisons were significantly different ($p<0.05$), except for the difference between the perceived location of peaks in the Low and High Contrast conditions.

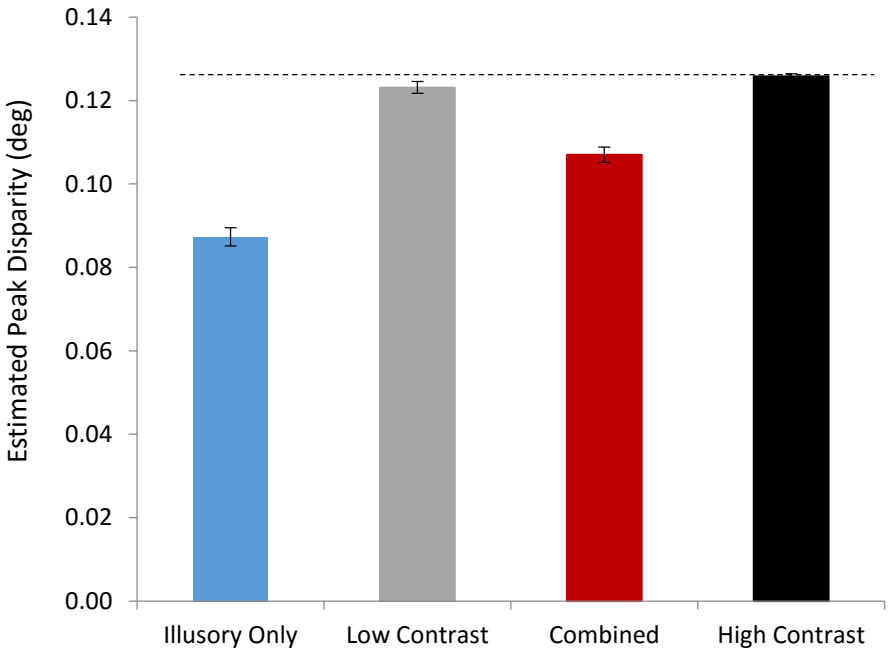

Figure 4.3. Average peak disparity (n=6) for each of the four stimulus conditions: Illusory Only (blue), Low Contrast (grey), Combined (red), and High Contrast (black) for the fused standard. The horizontal black dotted line represents the luminance-defined disparity at the peak of the luminance template. Error bars represent one standard error of the mean.

First, the comparison of the perceived location of surface peaks defined by luminance edges only (i.e. High & Low Contrast conditions in Figure 4.3) revealed that there was no difference in the magnitude of the perceived peaks. Importantly, the estimated disparity of the perceived peak in the high and low contrast surfaces matched the luminance-defined disparity present at the surface peak. This confirmed that the observers' depth estimates of the luminance-defined surfaces were accurate and the disparity probe did not introduce a bias[2]. Further, the results show that observers could precisely localize the perceived location of peaks in these luminance-defined surfaces.

In the Illusory Only condition (blue) in Figure 4.3, it appears that the illusory surface was consistently interpolated to a shallower peak than the perceptually equated luminance surface. This was confirmed by the statistically significant difference between the Illusory Only and Low Contrast condition ($p<0.001$). Therefore, the interpolation of the disparity signal along the illusory boundary followed a shallower trajectory than the sinusoidal luminance-defined template. This result echoes that of Warren, Maloney, and Landy (2002) who showed that disparity interpolation does not necessarily follow a parabolic contour. Instead it appears from their data that the 'human visual spline' fits a different class of curves than were used to generate the stimuli.

The estimates in the Combined condition (red) in Figure 4.3, were significantly different from estimates in both the Illusory Only and Low Contrast conditions ($p<0.05$). The combined peak was consistently localized in between the Illusory Only and Low Contrast surface peaks. When the surface was defined by luminance edges that occluded the inducing elements, the perceived location of the peak was strongly influenced by the presence of the occlusion geometry

[2] To eliminate the possibility of an effect of contrast polarity, a control task with a subset of observers (n=3) was performed comparing the perceived peak of a high contrast white surface to the black surface used in Experiment 4.2. There was no significant difference in the magnitude of the peaks.

at the inducing elements. It appears that the presence of the inducers consistently reduced the perceived depth at the peak of the surface, even in the presence of a luminance-defined signal that, in isolation, was consistently localized to a larger peak disparity.

4.5.2 Diplopia Standard

Not only did the estimated disparity of the peak increase at the diplopia point (relative to the fused reference), the relative locations of the surface peaks changed as well. The mean disparity estimates in Figure 4.4 (individual psychometric functions can be found in Appendix C) revealed that the perceived locations of the Illusory Only, Combined, and Low Contrast surface peaks were matched to a shallower probe disparity than in the High Contrast condition ($p<0.001$). In fact, all pairwise comparisons at the diplopia threshold were significantly different ($p<0.05$).

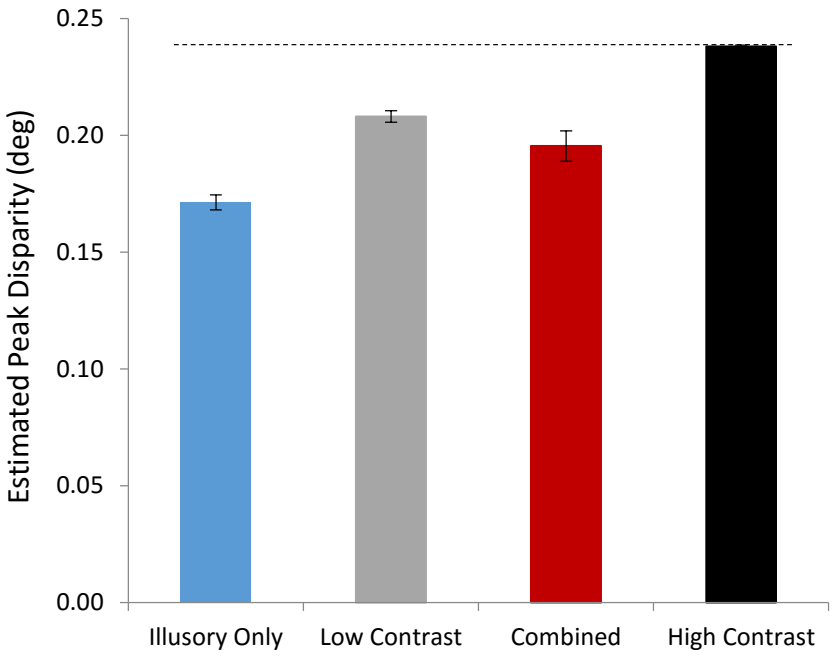

Figure 4.4. Average peak disparity (n=6) for each of the four stimulus conditions: Illusory Only (blue), Low Contrast (grey), Combined (red), and High Contrast (black) for the diplopia standard. The horizontal black dotted line represents the relative disparity at the peak of the luminance-defined template. Error bars represent one standard error of the mean difference between each condition and the High Contrast condition. Thus, the between-subject variation in diplopia points is removed from the error term.

When the inducing edge was presented at the diplopia point, there was a significant difference between the perceived locations of the peaks in the High and Low Contrast conditions that was not seen when the standard was fused. While the perceived height of the high contrast peak was consistent with the disparity along the luminance-defined edge, the low contrast peak was perceptually shallower. The fact that this difference in perceived amplitude of the surface was not evident when the stereopairs were fused confirms that the interpolation process was disrupted at the diplopia threshold.

As in the fused range, disparity matches in the Combined condition using diplopic stimuli were consistently between the Illusory Only and Low Contrast estimates (Figure 4.4). The perceived height of the peak in the combined condition was significantly different from both the

illusory (p=0.006) and low contrast peaks estimates (p=0.029). However, unlike the fused range, there were substantial interobserver differences in the perceived location of the peak at the diplopia threshold for this condition (red bar in Figure 4.4). That is, half of the observers perceived the peak at the same disparity as the Illusory Only function, while the other half perceived the peak at a disparity similar to the Low Contrast function (see Appendix C for individual differences). This suggests that reducing the reliability of the disparity signal changed how the depth information from disparity and the occlusion features were combined to determine the shape of the 3D surface.

4.6 Discussion

4.6.1 Do Illusory Boundaries Interpolate to a Shallower Surface at the Diplopia Point?

To test my initial hypothesis that the illusory surface would interpolate to a shallower surface when the inducing edge was near diplopia, I compared the differences in the perceived peak height in the illusory and luminance surfaces when fused vs. diplopic. The mean difference between the perceived location of peaks in the illusory and high contrast fused conditions was approximately 0.039deg, while the difference at the diplopia threshold was 0.067deg. At first glance, it appears that the illusory surface was indeed interpolated to a shallower surface when the disparity was large. However, the comparison of the perceived location of the illusory surface peak to the luminance-defined disparity at the tip of the inducing elements (0.087deg) revealed that the peak of the surface was remarkably close to the disparity at the tip of the inducing edge for the fused standard (0.088 SE= ±0.003deg). A similar pattern of results was seen at the diplopia threshold where the estimated disparity of the illusory peak was approximately 0.01deg (SE=±0.004deg) above the disparity at the tip of the inducing edge. Regardless of the magnitude of disparity along the inducing edge, the illusory peak was consistently localized to a disparity

equivalent to the relative disparity at the tip of the inducing edge. It is possible that the trajectory of the disparity interpolation from the inducing edge was not as flexible as initially hypothesized. Instead it appears that the combination of depth cues at the inducing edge constrained the surface peak to a location equivalent to the largest disparity in the inducing region. This issue is discussed further in Section 6.3.

4.6.2 Differences in the Depth Magnitude Task

The results of the disparity probe task used above shows clear, reliable differences in percepts of surfaces defined by luminance and illusory boundaries. However, no such differences were seen in Experiment 4.1 where depth magnitude estimates were recorded. I attribute this difference to the precision of the tasks used in these two studies. That is, the large variability in perceived depth magnitude estimates in Experiment 4.1 made it difficult to detect these differences. I tested this hypothesis by examining the standard deviation (SD) of the mean differences between our stimulus conditions in the depth magnitude and disparity probe datasets and approximating the SD required to detect the differences using a conventional power analysis.

Table D.1 (see Appendix D) compares the individual difference in the fused range between estimates of the illusory peak to the low contrast and combined conditions in the depth magnitude and disparity probe datasets. To determine if the variance in the depth magnitude dataset was too large to detect the differences between test conditions, I calculated the SD that would be necessary to detect these differences. Assuming that the perceived differences in the disparity probe dataset were the true differences I was trying to detect, I used the power.t.test function (pwr package) in R to calculate the required SD (Cohen, 1988). In the disparity probe dataset, the $SD_{observed}$ of the difference between the illusory and combined conditions, and the illusory and low contrast conditions were 0.8 and 1.1, respectively. In the depth magnitude

dataset, the standard deviations were much larger ($SD_{observed}$=4.5 and 3.2, respectively). The actual differences in perceived peak height observed in the disparity probe paradigm were 3.09mm for the illusory and combined conditions, and 5.64mm for the illusory and low contrast conditions. To detect these differences using a t-test, the $SD_{required}$ must be smaller than 2.2 and 3.9, respectively (assuming α=0.05, and *power*=0.8). As expected, the $SD_{observed}$ in the disparity probe data was more than precise enough to detect these differences ($SD_{observed}$=0.8 and $SD_{observed}$=1.1, respectively). However, in the depth magnitude dataset the $SD_{observed}$ of the differences between the illusory and combined conditions was much too large to detect the actual difference ($SD_{observed}$=4.5). The $SD_{observed}$ of the difference between the illusory and low contrast conditions ($SD_{observed}$=3.2) was just below the SD necessary for detection ($SD_{required}$=3.9). Even though the $SD_{observed}$ above was less than the $SD_{required}$, the fact that the depth magnitude analysis collapsed the three stimulus conditions into a single variable, the combined variance was likely too large to achieve significance. Thus, the small differences (under 6mm) between test conditions detected in the disparity probe data were much too small to be detected given the large variance in the depth magnitude data.

4.6.3 Reduction of the Perceived Peak

Observers could precisely localize illusory contours with the same (if not better) precision as a perceptually equated luminance edge. One surprising result was the degree to which the inducing elements reduced the perceived depth of the low contrast luminance-defined surface peak. Why would the presence of the features necessary for illusory boundary formation strongly influence the perceived location of the surface peak when there was a suprathreshold luminance-defined disparity signal present? One possibility is that the shape information provided by the occlusion features and disparity signal at the inducers was more reliable than the disparity-

defined peak of the low contrast luminance edge. As a result, when the interpolated surface was shallower, it was more stable. If this is true, then estimates of the illusory surface peak should be more precise than the perceptually equated luminance-defined surface. In Chapter 5, I evaluated this hypothesis by measuring observers' ability to discriminate the perceived depth at the peak of these surfaces.

Chapter 5

5.1 Introduction

While previous research has emphasized that illusory boundaries generated by Kanizsa configurations share neural resources and perceptual effects with luminance-defined edges (Fahle & Palm, 1991; Larsson et al., 1999; von der Heydt, 1984), an observer's ability to discriminate the orientation of the two contours varies with the configuration. For example, Westheimer and Li (1997) compared the orientation discrimination thresholds for 2D square Kanizsa figures with illusory or luminance-defined contours. They found that observers' thresholds for illusory contours were higher than for luminance-defined contours by a factor of 2. Similar differences in orientation thresholds are seen for illusory boundaries generated by line terminations (Vogels & Orban, 1987). When observers judge the shape of an illusory surface defined by only 2D occlusion geometry, their discrimination thresholds are higher than observed when the surface is defined by a luminance edge. It is important to note that the 3D curved surfaces used in the current paradigm contain both 2D and 3D (binocular disparity) shape information.

Several studies have evaluated the reliability of disparity as a cue to surface shape. In particular, studies of surface slant have evaluated how changes in viewing distance affect the reliability of shape from disparity judgements. For example, the variability of disparity-based

slant estimates increases by more than a factor of 10 when the viewing distance is increased from near space up to 120cm (Banks, Hooge, & Backus, 2001). In addition, while stereoscopic slant discrimination thresholds generally increase as the magnitude of surface slant increases (Knill & Saunders, 2003), there are large interobserver differences. The reliability of depth percepts from stereoscopically defined curved convex surfaces has not received as much empirical attention as the perception of slanted surfaces. One notable example is Johnston's (1991) study in which she assessed depth constancy using random-dot cylindrical surfaces. Her results showed that depth estimates were systematically distorted as function of viewing distance. Similar studies found low thresholds for the discrimination of curved surfaces, but they also report large biases in perceived shape (Brenner & van Damme, 1999). Generally, disparity thresholds for 3D curved luminance-defined surfaces show a gradual increase as the disparity along the contour increases, especially once the edge is perceptually diplopic (Vreven, McKee, & Verghese, 2002). In sum, despite the large interobserver differences in the reliability of perceived depth for stereoscopically defined curved surfaces, binocular disparity on its own can reliably define surface shape if the stimulus is presented at relatively short viewing distances.

However, the relationship between stereoscopic and monocular judgements of position depends on the task and stimulus configuration. That is, in configurations with sparse isolated targets on the fixation plane, judgements of position based on binocular disparity can be superior to monocular judgements (McKee et al., 1990). While in other configurations, lateral position judgements along the x-axis have been shown to be better than depth interval judgements along the z-axis (McKee, Levi, & Bowne, 1990). The precision of depth estimates has not been assessed for stereoscopically defined illusory figures like those used here. By measuring the precision of depth estimates of illusory and luminance-defined surfaces, I evaluated whether the differences in the location of the perceived peaks in Experiment 4.2 were due to the relative

reliabilities of the two surfaces. Careful control of the stimulus configuration (as described in Experiment 4.2 above) permitted the direct comparison of performance. If estimates of the illusory surface are indeed more reliable than the perceptually equated luminance edge, then the strong influence of the inducing elements on the perceived peak in Experiment 4.2 was due to the fact that the occlusion and disparity cues at the fused inducing element were consistent with a shallower, more reliable illusory surface.

5.1.1 Rationale

In this experiment, I measured the relative precision of observers' ability to localize the illusory and luminance-defined surface peaks. I used a 2IFC paradigm with a method of constant stimuli in which observers judged the relative depth between the frontoparallel plane containing the inducing elements and the peak of the curved surface. From the psychometric data I computed the just-noticeable difference (JND) for each stimulus condition. This value represents the smallest change in the relative disparity at the tip of the vertical inducing edge necessary for observers to perceive a change in the depth at the surface peak. Comparison of JNDs obtained using illusory and luminance-defined surfaces can reveal if observers can discriminate the perceived peak of interpolated illusory surfaces as precisely as a surface defined by low contrast luminance edges. If the presence of the inducing elements reduced the perceived location of the peak in the combined surface because the local shape information at the inducers was more reliable, then the JND of depth judgements of the illusory surface should be smaller than the low contrast luminance-defined surface. In addition, I predicted that the interobserver differences in the perceived location of the peak in the combined surface at the diplopia threshold were due to the reduced reliability of the signals. Thus, there should be little to no difference between the JNDs of the illusory and low contrast surfaces at the diplopic threshold.

5.2 Methods for Experiment 5.1

Observers

The observers that participated in this experiment are described in Section 1.6.1.

Stimuli

The four surface conditions described in Experiment 4.2 were used here (i.e. Illusory Only, Combined, Low and High Contrast). As in the preceding experiment, these conditions were tested using both a fused and diplopic standard. The stimuli were generated as described previously, and presented along with the fusion field as illustrated in Figure 3.1. The inducer disparity values used in each condition were sampled symmetrically around the two standards used in Experiment 4.2 (i.e. fused or diplopic). The fused standard was the same for all observers with a relative inducer disparity of 0.09deg between the tips of the vertical inducing edge. The figures were presented with one of nine crossed inducer disparities (0.03, 0.04, 0.06, 0.07, 0.09, 0.10, 0.12, 0.13, or 0.14deg) with a step size of 0.02deg from the fused standard. In the diplopic condition, the standard was presented at the inducer diplopia point previously calculated for each observer (see Chapter 3). The figures were displayed with one of nine crossed inducer disparities with a 0.02deg step size, above and below the standard (i.e. -4, -3, -2, -1, diplopic standard, +1, +2, +3, +4 pixels). Thus, the same step size was used for all observers, but the reference disparity was determined by their individual diplopia point.

Apparatus

The apparatus was the same as described in Section 1.6.3.

Procedure

The JND for each stimulus condition was measured using a 2IFC paradigm and the method of constant stimuli. The standard was randomly presented in the first or second interval,

while the other surface was presented in the other interval at one of the nine test disparities. The duration of each interval was 320ms with a 750ms inter-stimulus interval during which they viewed a Nonius cross to realign their eyes. The four stimulus conditions were assessed in separate blocks and in each block the nine test disparities were randomly presented 30 times, for a total of 270 trials per condition. Each observer completed the four conditions at both the fused and diplopic standards for a total of 8 test conditions. The test order was randomized across observers and between each block of trials observers had a short break. On all trials observers were asked to indicate which of the two surfaces had more depth between the plane with the inducing elements and the peak of the surface. Observers pressed one of two gamepad buttons to indicate either "interval 1" or "interval 2." Prior to each test session observers performed a brief practice session of 4 trials at each test disparity to familiarize themselves with the stimuli and task.

5.3 Results and Discussion

Psychometric data was fit using a cumulative Gaussian and the JND was computed for each condition at both the fused and diplopic standard for all observers (n=7). An example of an observer's psychometric data can be seen in Figure 5.1. The analysis was performed in R using glm() function in the R stats package. Bootstrapped confidence intervals were calculated using Monte Carlo simulations methods run 1,000 times for each dataset (Wichmann & Hill, 2001a, 2001b). These JNDs represent the smallest amount of inducer disparity necessary for observers to perceive a change in the depth at the surface peak. One observer was removed from the final analysis because they performed at chance levels in the Low Contrast condition in both the fused and diplopic range.

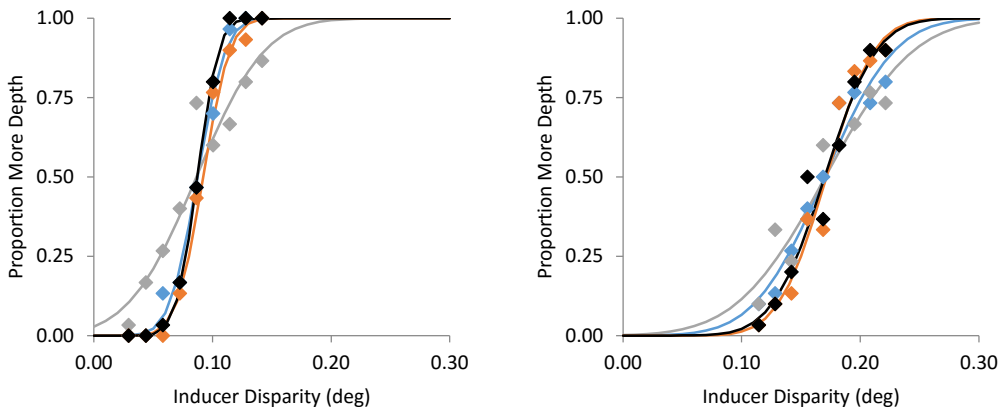

Figure 5.1. An example of an observer's psychometric data plotted as a function of inducer disparity in degrees. The illusory (blue), low contrast (grey), combined (red), and high contrast (black) conditions are shown for conditions with fused and diplopic standards (left and right plot, respectively).

To assess the differences in precision between stimulus conditions a repeated-measures analysis of variance compared the effect of Stimulus Configuration and Disparity Range on JND. The analysis revealed a significant effect of Stimulus Configuration, $F(3,15)=12.67$, $p<0.001$, $\eta^2=0.37$, Disparity Range, $F(1,5)=15.32$, $p=0.011$, $\eta^2=0.26$, but no significant two-way interaction, $F(3,15)=1.38$, $p=0.29$, $\eta^2=0.06$. The significant effect of Stimulus Configuration and Disparity Range in the preceding analysis suggests that precision estimates differed between our stimulus conditions *within* the fused and diplopic range. The lack of an interaction indicates that while the mean JND at the diplopic threshold was elevated compared to the fused range, the difference was not dependent on the surface configuration. To examine the relationship between the stimulus configurations more closely I used pairwise t-tests and Benjamini and Hochberg's (1995) method for controlling false discovery rates. In the fused range, the Low Contrast condition had a significantly larger JND than the Illusory Only ($p=0.024$), Combined ($p=0.024$), and High Contrast conditions ($p=0.026$). At the diplopia threshold, the mean JND in the Low

Contrast condition was significantly larger than the mean JND in the High Contrast condition ($p=0.018$), and no other within-group contrasts were significant ($p>0.05$).

5.3.1 Fused Standard

The mean JND for each stimulus condition when the standard was fused are plotted in Figure 5.2. The JNDs were consistently small which demonstrates that observers precisely estimated the perceived depth at the surface peak for all stimuli. For example, when the inducers were fused, observers were able to perceive a change in the depth of the surface peak with only a 0.02deg change in the relative disparity at the tip of the vertical inducing edge. Further, despite the absence of features within the central region of the illusory surface, observers' estimates were equally precise in the illusory and high contrast luminance conditions. These results, combined with the precision data reported in Experiment 4.2 further establish that curvilinear surfaces defined by illusory contours form a consistent, reliable 3D shape (Carman & Welch, 1992).

Importantly, these results show that precision was poorer in the low contrast luminance condition than in any other surface condition; thus, as predicted, the shape of the surface was less reliable in the low contrast condition than it was in the illusory condition. Further, if the addition of the fused inducing elements to the luminance-defined surface strongly influences perceived location of the peak by creating a more stable surface configuration, then the JND of the combined surface should be similar to the JND of illusory surface. In Figure 5.2, it is clear that this is indeed the case. When a low contrast luminance surface occludes the fused inducing elements (i.e. combined surface) observers could reliably localize the position of the perceived peak as precisely as a surface defined only by illusory boundaries. The similarity of the reliability of the estimates of the illusory and combined conditions suggest that the presence of occlusion

features and high contrast disparity signal at the fused inducers improved the precision of depth estimates to a level obtained using a salient, high contrast luminance-defined surface.

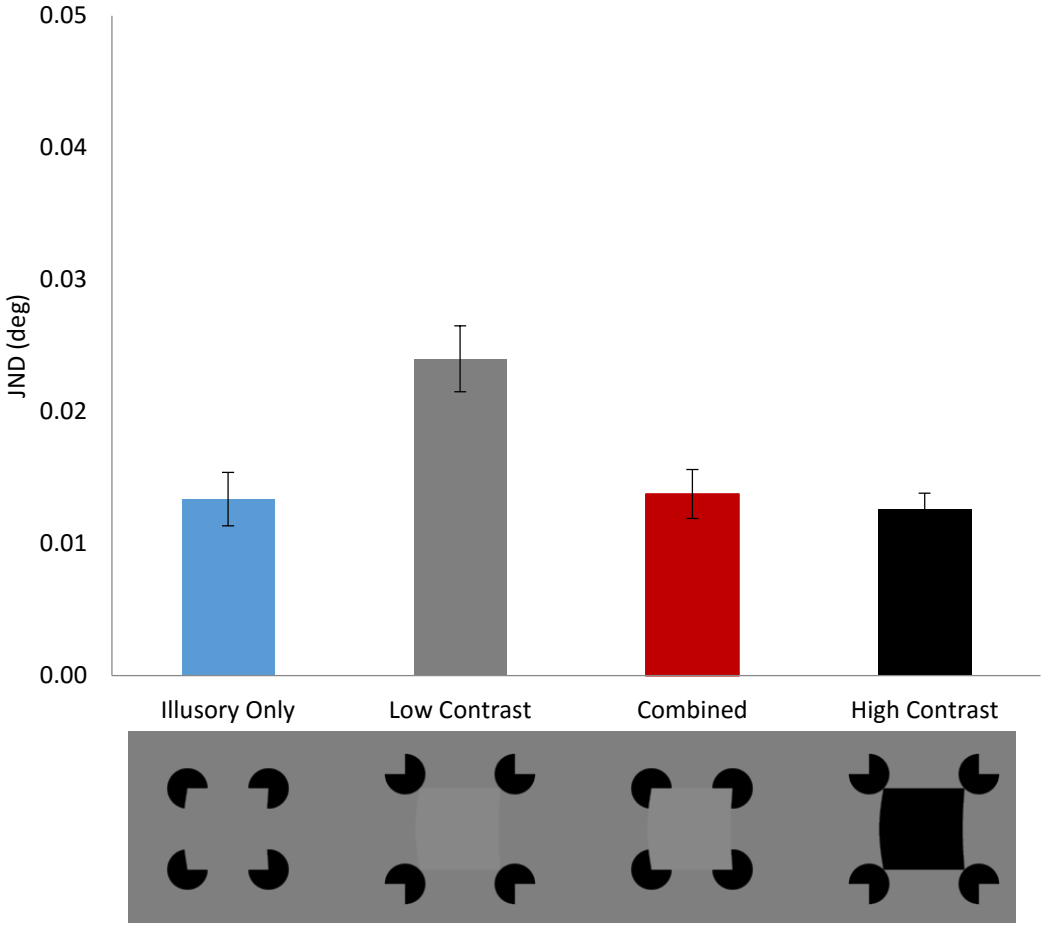

Figure 5.2. The average JND for each stimulus configuration in the fused range for the four stimulus conditions: Illusory (blue), Low Contrast (grey), Combined (red), and High Contrast (black). Error bars represent one standard error of the mean.

5.3.2 Diplopic Standard

As expected the JNDs for all surface conditions were elevated when the reference disparity was at the diplopia point (relative to the fused condition above). These results confirm that this manipulation was effective in reducing the reliability of the disparity signal. In addition, there was higher within and between subject variability when the inducer disparity was at the diplopia point. At the diplopia threshold, when the disparity information at the inducing edge was

less reliable, the JNDs were similar across the surface configurations; the only significant difference was between the low and high contrast luminance-defined surfaces (Figure 5.3). Compared to results obtained with fused stimuli, at the diplopia threshold there was no longer a difference in the precision of depth estimates between the illusory, low contrast, and combined surfaces. Recall in Experiment 4.2, there were interobserver differences in the perceived location of peaks at the diplopia threshold. As shown in Figure 5.3, it is clear that there was no longer an advantage of the illusory boundary over the perceptually equated luminance edge. As a result, the interobserver differences in the peak of the combined condition were due to individual differences in how the shape information at the inducing region (occlusion and disparity) was combined when one of these cues was less reliable (i.e. disparity in this case).

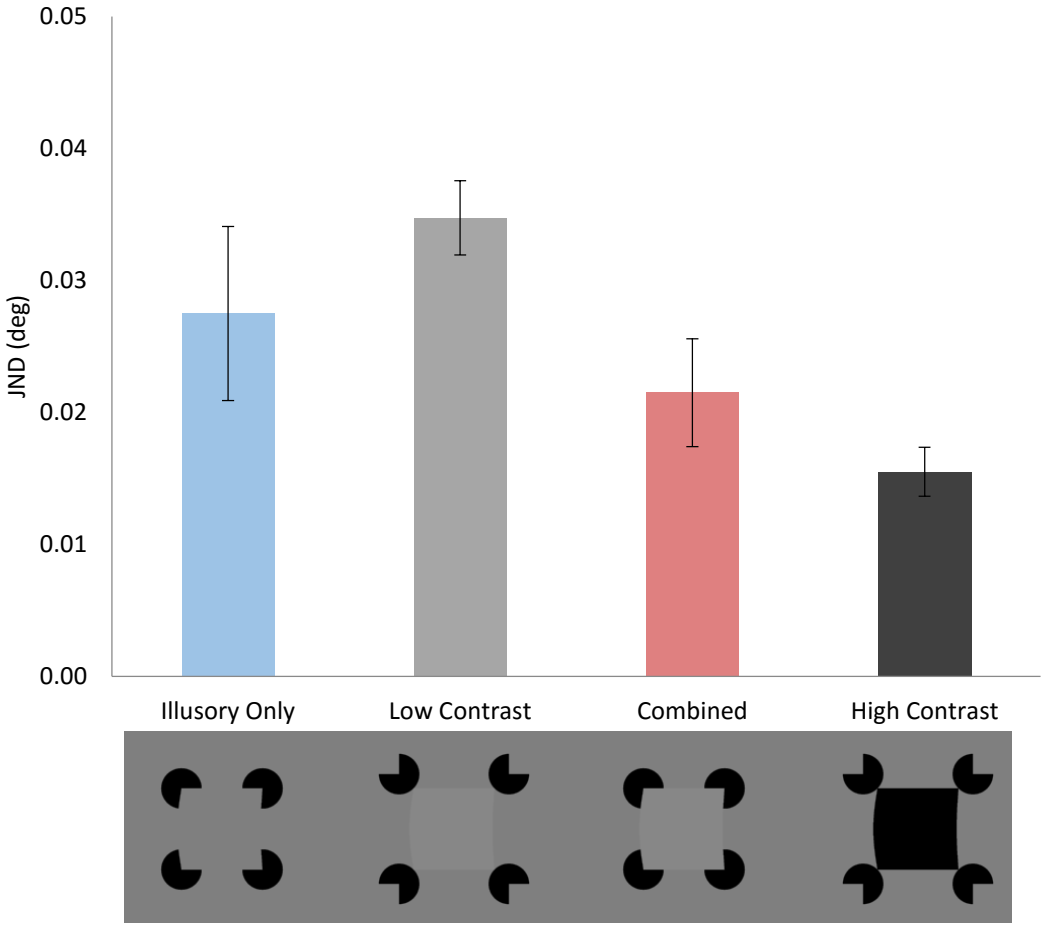

Figure 5.3. The average JND for each stimulus configuration at the diplopia threshold for the four stimulus conditions: Illusory (blue), Low Contrast (grey), Combined (red), and High Contrast (black). Error bars represent one standard error of the mean.

Taken together the results of Experiment 4.2 and 5.2 confirm that the presence of the ordinal depth signal provided by occlusion features at the inducing elements plays an important role in depth processing. The addition of the occlusion features at the inducers has a strong impact on the quantitative depth provided by the disparity signal along the vertical surface edge. In the fused range, when a luminance-defined surface occluded the inducing elements, depth estimates were influenced by both the explicit luminance-defined disparity signal and the occlusion features. The presence of the fused inducing elements consistently reduced the perceived location of the peak of the surface despite an alternative luminance-defined disparity

signal at the surface peak. The combination of the shape information (occlusion features and disparity signal) at the fused inducing elements was more reliable compared to the low contrast luminance signal that defines the surface edge (defined by disparity). At the diplopia threshold, when both the inducing elements and an alternative luminance-defined disparity signal were present, but less reliable, perceived depth estimates appeared to be dominated by one source or the other. Despite the presence of an alternative luminance-defined signal, the presence of the inducing elements consistently influenced the perceived depth of stereoscopic surfaces. These results could be the consequence of the combination of quantitative (disparity) and qualitative (occlusion and luminance) depth cues that define the shape of these stereoscopic surfaces. Previous cue combination studies have demonstrated that qualitative depth cues, such as familiarity, convexity (Bertamini, Martinovic, & Wuerger, 2008; Burge, Peterson, & Palmer, 2005), and focus cues (Watt, Akeley, Ernst, & Banks, 2005) influence perceived depth from disparity. In the following section, I assessed whether the perceived depth of the combined surface was consistent with the linear combination of illusory and luminance-defined depth signals.

5.4 Cue Combination

5.4.1 Introduction

The pattern of results in Experiment 5.1 suggest that observers combined depth information in the stimuli based on the relative reliability of the individual depth cues as predicted by a cue combination model. I assessed this possibility by determining if the magnitude and precision of depth estimates in the combined surface condition were combined as predicted by a maximum likelihood linear cue combination model. There is a possibility that illusory boundaries were formed in the combined surface condition. Despite the tendency for luminance-

defined elements to weaken illusory boundaries when they are inconsistent with or superimpose the illusory geometry (Gilliam & Nakayama, 2002; Kanizsa, 1979; Ringach & Shapley, 1996), there is some evidence of a perceived brightness enhancement in the combined surface condition that suggests illusory boundaries were present; however, if they did occur they were very weak. Even though the perceived depth in these surfaces were likely the result of the underlying cues from binocular disparity, occlusion, and luminance features, to simplify the comparison I described the combined surface as the combination of the depth from illusory and luminance-defined boundaries.

5.4.2 Linear Cue Combination

To assess the influence of the illusory and low contrast luminance-defined boundaries on the shape of the combined surface, I examined the individual contribution of each contour using maximum likelihood linear cue combination model for maximum reliability. This model assumes that the integration of two cues is optimal when observers attempt to minimize the variance of their depth estimates. Thus, the cue weights are proportional to the cue's reliability (Equation 1), which is the inverse of the variance of that cue (Cochran, 1937).

$$r_i = {}^{1}\!/_{\sigma_i^2} \tag{1}$$

In addition, this model assumes that the underlying estimates were unbiased, that is the cues were normally distributed and conditionally independent (Landy, Maloney, Johnston, & Young, 1995). The model is defined as:

$$\hat{d} = w_I d_I + w_L d_L \tag{2}$$

Where,

$$w_I = r_I/(r_L + r_I) \quad (3)$$

$$w_L = r_L/(r_L + r_I)$$

Where, d_I and d_L are the perceived location of the peak of the surface defined by illusory and low contrast luminance edges, respectively. The weights, w_I and w_L are calculated from the variance of the estimates for the illusory surface, σ_I^2 and low contrast luminance surface, σ_L^2. In a simple linear cue combination model, the weights (w_I and w_l) are assumed to be proportional to the inverse of the variances ($\sigma^2{}_I$ and $\sigma^2{}_L$) of the cue distributions, so greater weight is placed on the more reliable cues (Ernst & Banks, 2002). This produces a combined estimate with a lower variance than any of the single-cue estimates. Thus, by combining the information from several depth cues the visual system can estimate the perceived depth with greater precision than it can by relying on any single cue (Ernst & Banks, 2002; Knill & Saunders, 2002; Landy et al., 1995).

5.4.3 Our Model

In the model used here, the variances of the illusory and luminance-defined depth estimates were determined by the 2IFC discrimination task in Experiment 5.1 and the mean of those depth estimates were the PSEs calculated in Experiment 4.2 (see Hillis, Watt, Landy, & Banks, 2004). To evaluate the contribution of illusory and luminance-defined signals to the perceived depth of the combined surface, the average PSE_i and σ_i was calculated for the illusory, low contrast luminance, and combined surfaces ($PSE_I\ \sigma_I$, $PSE_L\ \sigma_L$, and $PSE_C\ \sigma_C$, respectively). The optimal linear model in Equation 2 was fit to each observer's dataset, resulting in an optimal PSE_{opt} and σ_{opt} for each observer (n=5). The mean of the observed and predicted sigma values can be seen in Figure 5.4.

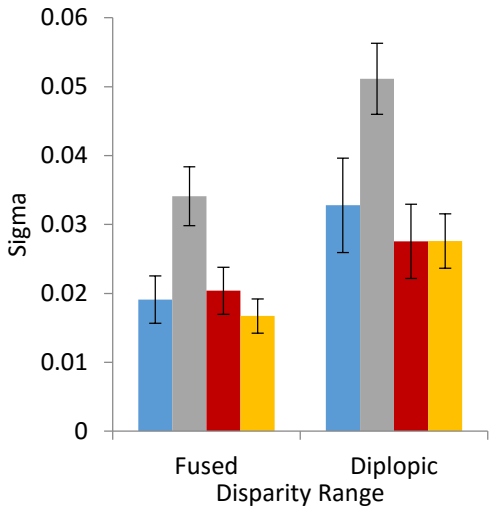

Figure 5.4. Average sigma values for perceived depth estimates of the illusory (blue), low contrast luminance (grey), and combined surfaces (red). The predicted sigma value (yellow) is calculated from the linear cue combination model in Equation 2. Error bars represent one standard error of the mean.

Comparison of the observed σ_c (red) to the predicted σ_{opt} (yellow) in Figure 5.4 revealed that the SD of observers' depth estimates in the fused range was consistent with an optimal linear cue combination. Examination of individual SDs revealed that the majority of observers (3 of 5) were highly consistent with the predicted sigma values while the remaining observers demonstrated slightly larger SD than predicted. However, while the diplopic range revealed a similar overall pattern, relative to the fused data there was greater variability in the SD of depth estimates. This could be due to the increased noise in the diplopic stimulus, and/or it could indicate that another combination rule was being applied. The differences in reliability of the individual cues are supported by the interobserver differences in the observed PSE for depth estimates of the combined surface in Experiment 4.2. The depth of the combined peak varied between observers at the diplopia threshold, whereby some observers perceived the combine peak at the same disparity as the low contrast luminance edge while others perceived the peak closer to the peak of the illusory surface (Appendix C).

I assessed if the observed PSEs were consistent with the predictions of the linear model by comparing the correlation between observed and predicted PSEs (Figure 5.5). The observed PSEs in the illusory ($t(8)=16.79$, $p<0.0001$, $r=0.99$), combined ($t(8)=23.24$, $p<0.0001$, $r=0.99$), and low contrast conditions ($t(8)=3.63$, $p<0.007$, $r=0.79$) were all highly correlated with the predicted PSEs from our model. Both the illusory and combined surface conditions closely followed predicted values ($R^2_{adj}=0.97$ and 0.98, respectively). While the correlation was still highly significant in the low contrast condition, the proportion of variance explained by the model was slightly less compared to the illusory and combined conditions ($R^2_{adj}=0.58$). As shown in Figure 5.5, the variability of both the observed and predicted PSEs increased in the diplopic range. Again, this was likely due to the decreased reliability of the disparity signal in the diplopic range.

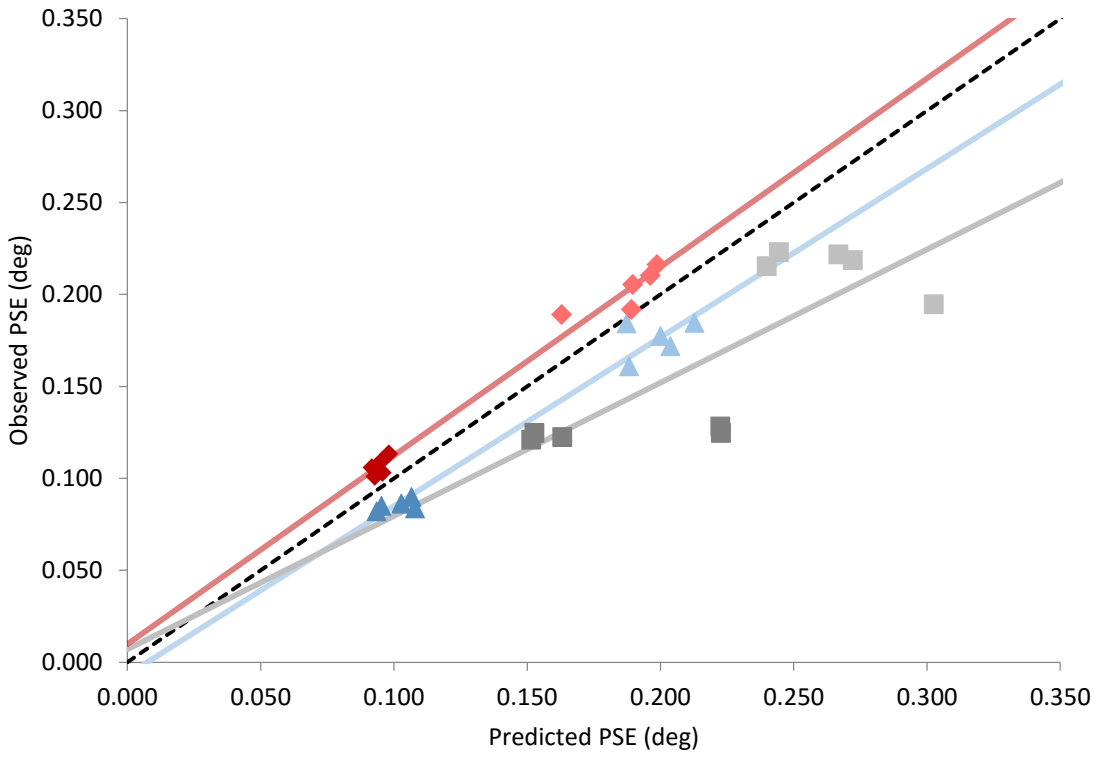

Figure 5.5. Observed PSEs for the illusory (blue triangles), low contrast luminance (grey squares), and combined surfaces (red diamonds) plotted as a function of the predicted PSE from the optimal linear model (Equation 2). In each condition, the darker and lighter symbols represent the data from the fused and diplopia standard, respectively. The black dotted line represents the theoretical PSEs predicted by the optimal linear model.

While our results were strongly correlated with predictions from a linear cue combination model, we should be cautious when interpreting the results. Given that the observed estimates were only measured at two disparities (i.e. a fused and diplopic standard); a linear model is more likely to be a good fit since these data were only sampled at two data points. If a more complex non-linear model actually described the relationship within the data, it would be necessary to sample a minimum of three points. In Figure 5.5, the observed estimates do appear to deviate from linear predictions. A repeated-measures analysis of variance confirmed that the observed PSEs significantly deviate from the predicted values within the three stimulus conditions,

$F(2,8)=14.96$, $p=0.002$; $\eta^2=0.51$. Pairwise t-tests confirmed the difference between observed and predicted values were highly significant for all three surface conditions ($p<0.001$).

Despite the apparent consistency of variances with those predicted by a linear combination model in Figure 5.4, the observed PSEs exhibited a systematic bias in which the means of the individual cue conditions (illusory and low contrast) were underestimated, while the combined estimates appeared larger than predictions. This pattern was seen in both the fused and diplopic range. When the illusory and low contrast surfaces were combined into an intermediate surface, observers consistently underweight the contribution of the illusory boundaries compared to the perceptually equated luminance edge. One possible explanation is that illusory boundaries were biased towards a more conservative interpolation that reflects prior assumptions of surface shape. Previous studies have suggested that the visual system may have prior assumptions biased towards the simplest surface interpretation when an image is compatible with more than one interpretation; due to lack of explicit shape information or ambiguous disparity matching (Albert, 2001; Albert & Hoffman, 2000). This assumption could be learned by passively observing the frequency of surface representations (Nakayama & Shimojo, 1992) or patterns in local features, such as the probability of contour junctions their relationship with occlusion (Anderson & Julesz, 1995; Rubin, 2001). A consequence of this assumption could be that the illusory boundaries were underweighted to compensate. However, despite the plausibility of this explanation of the predicted PSEs, underweighting of individual cues could also be a consequence of the interactions between the depth cues (disparity, occlusion, and luminance) that underlie the perceived depth of the surface.

5.4.4 Alternative Cue Combination Models

While observers do appear to take into account the weights of the individual cues defined by the inverse of the variance, the underestimation of individual cues and overestimation of the combined estimate, suggest that they may not be combined linearly. This was likely due to the influence of other sources of depth information that were not accounted for in this simple model. All surface conditions were defined partly by disparity, but the luminance relationships and occlusion features vary between conditions. Since all surface variants share underlying depth cues there could be more complex interactions, such as correlation or non-independence in the errors of the cue distributions and possibly the interactions between individual cues could be non-linear (Oruç, Maloney, & Landy, 2003). Kogo et al. (2014) has recently proposed a non-linear dynamic weighting to describe the illusory depth elicited by the combination of occlusion cues and the depth from binocular disparity in Kanizsa configurations. They suggest that consistent cues may work together to enhance the depth perception of illusory surfaces and reduce the ambiguity of individual cues. Other studies have suggested that global geometry, such as the consistency of curvature defined by 2D or 3D cues may also factor into the integration of individual cues beyond a simple weighted linear summation (Stevens, 1991). It is possible that such interactions were present in our surface conditions that reflect non-independence between underlying depth cues.

To evaluate the contribution of the underlying depth from binocular disparity, occlusion features, and luminance relationships it would be beneficial to systematically vary the properties (i.e. separation, size, contrast, polarity) of the inducing elements and surface to assess the impact on the perceived depth of the surface peak. For example, a future cue combination paradigm could assess the perceived depth of the combined surface under a variety of luminance relationships while holding the depth from disparity and occlusion features constant. Given the potential of multiple interactions between underlying depth cues, this example above would

provide a way of systematically assessing the influence of luminance relationships at T-junctions while controlling the influence of other depth cues. This is important given the complexity of combining quantitative (disparity) and qualitative (occlusion and luminance) depth cues, as it is unclear how these two sources of depth information are combined (Landy, Maloney, Johnston, & Young, 1995). Typically studies examining the influence of quantitative and qualitative depth cues examine how these cues are combined when they are consistent or in conflict since the qualitative cues in isolation provide no additional numeric information. When the signals conflict there can be individual differences in the combination and interpretation of occlusion and disparity information (Cavanough, 1987). Previous research has shown that qualitative pictorial cues, such as convexity and familiarity can influence the perceived depth from disparity at large viewing distances (Bertamini, Martinovic, & Wuerger, 2008; Burge, Peterson, & Palmer, 2005). Neurons that are sensitive to border-ownership (i.e. figure-ground relationships) of occlusion junctions even show preference for stereo disparity that is congruent with the preferred side of the contour (Qiu & von der Heydt, 2005). However, it is unclear how these two sources of depth information are combined since these interactions could rely on quantitative or qualitative signals regarding depth relationships (Kogo et al., 2014). Thus, this initial cue combination analysis provides a starting point for the assessment of the combination of depth from disparity, occlusion features, and luminance relationships in stereoscopic Kanizsa figures.

Chapter 6

Discussion

6.1 Summary

The aim of this series of experiments was to understand the nature of the disparity signal that underlies the perception of illusory stereoscopic surfaces. To accomplish this, I evaluated the contribution of the conventional luminance-defined disparity at the inducing edge to the perceived depth of illusory surfaces by systematically varying the 2D and 3D properties of stereoscopic Kanizsa configurations. In Experiment 2.1, I introduced a novel approach to equate the salience of a stereoscopic luminance-defined surface to an illusory surface with equivalent disparity in the inducing region. In Experiment 3.1, I determined how to degrade the disparity signal without disrupting the illusory boundaries by presenting the stereoscopic illusory Kanizsa figures at each observer's diplopia point. In Experiment 4.1, I demonstrated that the magnitude of perceived depth in these surfaces demonstrates a consistent linear increase as a function of disparity with surprisingly little degradation of perceived depth in the diplopic range. Experiment 4.2 expanded on these results by illustrating that the addition of qualitative depth cues at the inducing elements critically impacts estimates of suprathreshold depth from binocular disparity. Experiment 5.1 confirmed my earlier hypothesis that the inclusion of the fused inducing edges forms a more reliable surface percept by increasing the precision of depth estimates of the surface peak. In addition, when the disparity signal was degraded (diplopia) there were interobserver differences in how the qualitative depth cues and depth from disparity were combined. Observers' perceived depth estimates appeared to systematically depend on the most reliable depth cue, but when depth from disparity was less reliable (diplopia) there were individual preferences for one cue over another and it was unclear how these two sources of depth information were combined. The linear cue combination analysis in Section 5.4 confirmed that observers took the variance of individual cues into account, but the method of combination may have been more complex than a simple linear model (i.e. non-linear or non-independent combination methods).

6.2 Contribution of 2D and 3D Illusory Boundaries

The original motivation of this series of studies was to evaluate if illusory contours provided a disparity signal that supports illusory surface formation. Given the results of Experiment 4.1, it was clear that the proposed paradigm would not be able to distinguish between these alternatives. Thus, I could not determine the individual contribution of the 2D and 3D illusory boundaries to the perceived location of the surface peak. I hypothesized that if the inducing edge was no longer perceptually fused, then the illusory percept would degrade, emphasizing the role of disparity interpolation in determining surface shape. However, none of the surface configurations in Experiment 4.1 demonstrated any loss of perceived depth, even at large inducer disparities. As discussed in Chapter 4, one factor that could have contributed to the robust percepts in the diplopic range was the presence of the separation information, which could have provided an additional cue that could be used to scale estimates of the perceived depth. However, this is an unlikely explanation given that the estimated depth increases smoothly across the test range (for discussion see Section 4.3.1). The continued increase in the perceived depth of the peak of the illusory surface, well beyond the diplopia point was surprising given that disparity interpolation is poorer for large edge disparities and tends to fail in stimuli with characteristics that are dependent on coarse stereopsis (Wurger & Landy, 1989). It is possible that the robust 3D surface perception was due to the presence of the supporting geometry of the 2D occlusion information and its interaction with the disparity signal (Anderson & Julesz, 1995). In these experiments I held the structure of the occlusion geometry constant (i.e. contrast, polarity, and/or orientation at junctions), so I could not identify the individual properties of the occlusion features that interacted with the disparity signal. However, the results of Experiment 4.1 prompted

subsequent evaluation of the way in which the 2D occlusion features modulate the use of disparity in defining 3D illusory surfaces.

6.3 Interpolation of Illusory Boundaries

6.3.1 Perceived Shape of Illusory Boundaries

The sparse central region in stereoscopic Kanizsa figures (Figure 6.1A) allows for multiple patterns of interpolation between adjacent inducing elements (Figure 6.1B). Previous investigation of the interpolation of illusory boundaries (Albert, 2001) and disparity interpolation (Grimson, 1981), suggest that the visual system tends to be very conservative when interpolating contours within ambiguous regions. Similarly, the current results demonstrated that the depth at the peak of curvilinear illusory boundaries was consistently shallower than the sinusoidal luminance-defined template used to generate the stimuli (Experiment 4.2). Comparison of the perceived location of the illusory surface peak to the luminance-defined disparity at the tip of the inducing elements revealed that regardless of the magnitude of disparity, the illusory surface peak was consistently localized to a disparity equivalent to the relative disparity at the tip of the inducing edge. These results echo the depth magnitude estimates in Experiment 4.1, where estimated depth was consistently 40% less than predicted from the binocular geometry at the peak of the luminance-defined template. Thus, regardless of the estimation method, the perceived illusory surface peak was highly influenced by the disparity signal at the tip of the inducing edge.

A

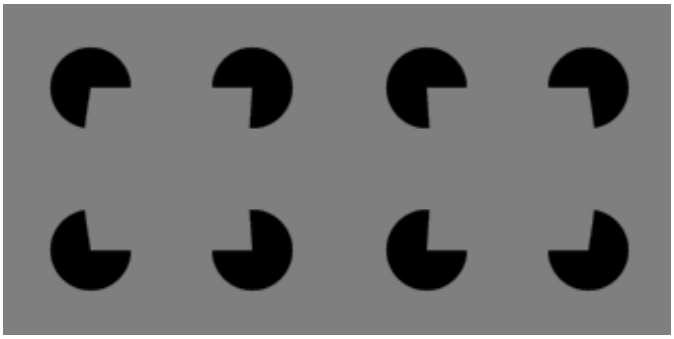

B

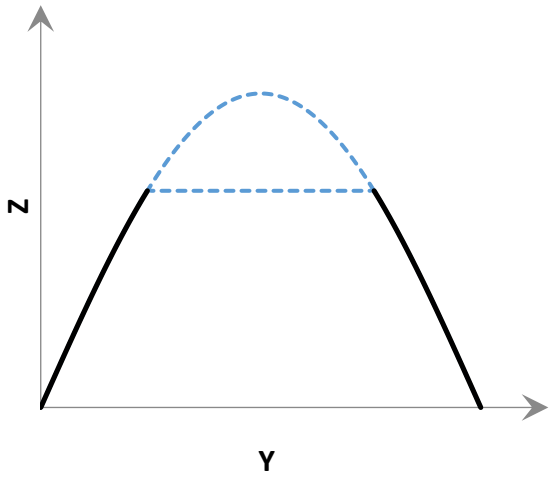

Figure 6.1. (A) An example of a stereoscopic Kanizsa figure used in the illusory condition. The right and left images are arranged for crossed fusion. (B) An illustration of the side-view of the stereoscopic illusory surface. The solid black lines represent the luminance-defined inducing edge. The curved dashed line represents the maximum interpolation according to the luminance-defined template. The straight dashed line represents the simplest possible pattern of interpolation directly in between the inducing elements. Note that although only select interpolation patterns are illustrated, intermediate patterns of interpolation are possible.

In the series of experiments reported here the perceived depth was measured at the illusory surface peak. It is possible that observers did not interpolate a curved surface, but instead interpolate a flat surface between adjacent inducing edges. As reported by others (Carman & Welch, 1992; Vreven, McKee, & Verghese, 2002) and in our preliminary observations, the interpolated surfaces consistently appeared curved. Moreover, in a brief follow-up experiment observers were asked to report the perceived shape of the surface configurations; observers consistently reported that they perceived a continuous curved illusory surface that reached a

maximum depth at a disparity equivalent to the relative disparity at the tip of the inducing elements. This suggests the interpolation profile was curved, but the height of the surface was greatly reduced compared to the template used to generate the stimuli. This reduction in curvature was likely due to the influence of the occlusion features, but further study is needed to understand this issue.

6.3.2 Occlusion Features and Disparity

Regardless of its shape, the depth defined by the disparity signal and occlusion features at the inducing region must be combined and interpolated across the ambiguous region to create a 3D stereoscopic surface. Anderson (2003) proposed that the presence of an occlusion edge imposes restrictions on the structure of disparity from local contrast signals that guide the visual system's computation of surface structure. The occlusion constraint is simply the fact that nearer surfaces tend to occlude more distant surfaces, and not the converse. This simple rule can have significant implications for the surface configurations that can arise from the local contours in each eyes image. Anderson proposed a simple principle called the 'contrast depth asymmetry principle' to describe how occlusion constrains disparity. He argues that the edges that generate the local contrast signals must be assigned distances that are greater than or equal to the disparity of that contrast signal. Thus, for a given luminance edge, if the disparity of the edge is crossed (closer in depth), only one side of the contour can be assigned to this depth; conversely, if the disparity is uncrossed (recedes in depth), both sides of the contour are constrained to appear at least this distance. This approach is useful to determine how the combination of the disparity signal and occlusion features creates stereoscopic illusory T-junctions that resolve the border-ownership (e.g. figure-ground) relationship by assigning the surface to the occluding edge (for details see Section 1.2). Similar guidelines have been proposed in studies of disparity

interpolation. For example, Mitchison and McKee (1987b) coined the 'nearest disparity rule' that states when a disparity signal is interpolated across an ambiguous region, the interpolated disparity tends to be equivalent to the disparity of the nearest unambiguous (i.e. matched) element. However, Anderson (2003) only applied this principle to frontoparallel Kanizsa configurations. The stereoscopic illusory surfaces used here contain disparity that varies continuously along the vertical inducing edge, but the results are consistent with Anderson's formulation and with Mitchson and McKee's proposal that the location of the illusory surface peak is consistently interpolated to a disparity equivalent to the relative disparity at the nearest luminance-defined element. The largest luminance-defined disparity present in the inducing region appears to constrain the maximum interpolated disparity.

6.3.3 Disparity Ownership

It could be argued that the pattern of depth magnitude data reported here may have been obtained without the interpolation of a stereoscopic surface; that is, that observers were simply basing their depth judgements on the maximum disparity associated with adjacent luminance-defined features. Indeed, as discussed above, studies of stereoscopic Kanizsa figures (Anderson, 2003), disparity interpolation (Mitchison & McKee, 1987b), and the current study all demonstrate that perceived depth estimates of ambiguous regions are highly constrained by the depth of adjacent luminance-defined elements. To evaluate this possibility, I conducted a follow-up experiment in which observers estimated the perceived depth magnitude of the inducer and the surface at the tip of the inducing element. If observers were basing their perceived depth estimates on the disparity at the tip of the inducing edge, then depth estimates of the inducer should always be equivalent to the perceived depth of the surface. In this study, five observers were asked to report the perceived depth of the inducer and surface at the tip of the inducing

element at three inducer disparities (0, 0.04, and 0.09deg). Observers were shown the stereoscopic Kanizsa figure for the same duration and under the same viewing conditions as described in Experiment 4.1; however, instead of using a sensor strip, observers made their estimates using a virtual ruler that appeared after stimulus presentation. On each trial they were asked to judge either the depth of the inducer or surface (text indicating the trial type, 'disk' or 'surface', was positioned below the stimulus).

The mean estimated depth of the inducer and surface are plotted as a function of inducer disparity in Figure 6.2. One observer was excluded due to a large overestimation at zero disparity. A repeated-measures analysis of variance revealed a significant interaction between the two conditions as a function of inducer disparity, $F(2,6)=20.75$, $p=0.002$, $\eta^2=0.42$. Pairwise comparisons with Benjamini and Hochberg's (1995) correction confirmed a significant difference in perceived depth between the two largest test disparities when estimating the depth of the surface ($p=0.049$), but no significant increase when estimating the depth of the inducer ($p=0.18$). Thus, not only were the perceived depth estimates larger when estimating the surface, the estimates showed a linear increase as a function of disparity while estimates of the inducer did not.

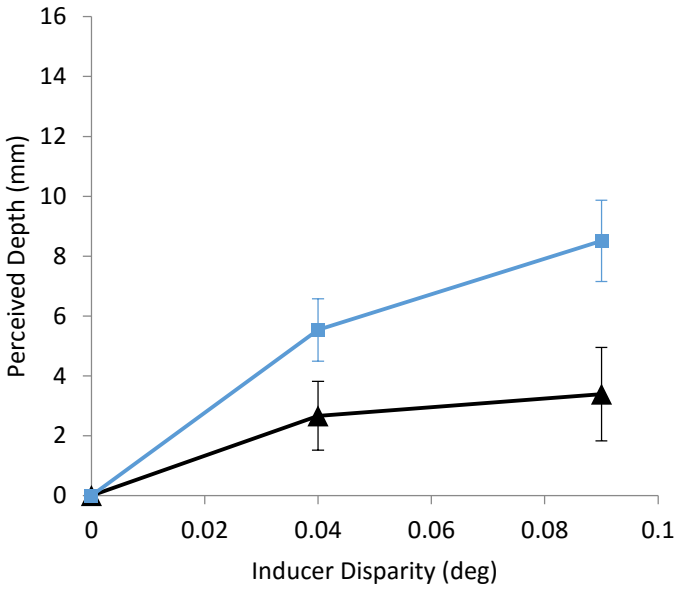

Figure 6.2. Mean depth estimates (n=4) for the inducer (black) and the surface (blue) at the tip of the inducing element. Error bars represent one standard error of the mean.

These results provide strong evidence that in fact observers do see a surface in these configurations, and that they judge its depth. Regardless of the magnitude of disparity along the vertical inducing edge, the depth of the high contrast inducer was near zero and demonstrated no increase as a function of disparity. Thus, observers were not basing their depth estimates on just the disparity at tip of the inducing elements, the disparity along the inducing edge was assigned to the illusory surface, not the inducing element. As discussed in Section 1.4, the relationship between the border-ownership defined by the 2D occlusion geometry and the direction of the depth defined by binocular disparity is critical to the formation of a stable 3D illusory surface (Anderson, 2003; Nakayama & Shimojo, 1992). The 2D border-ownership is resolved by the global occlusion geometry that assigns the horizontal and vertical inducing edges to the illusory surface and the outer edge of the disk to the inducer (Section 1.2). The results above demonstrate that this 2D border-ownership in combination with *disparity ownership* along the vertical

inducing edge is critical to defining figure-ground relationships. This conclusion is consistent with previous work by Kogo et al. (2014) who argued the fundamental role of 2D border-ownership in defining the depth and lightness percepts in illusory Kanizsa figures, in addition to the critical role of the combination of 2D occlusion geometry and binocular disparity in defining the perceived depth of the surface. Thus, the 2D occlusion geometry influences the disparity ownership of the boundaries and their combination defines the 3D figure-ground relationships between the surface and the inducing elements.

6.4 Combined Surfaces

6.4.1 Introduction

When an alternative, luminance-defined, disparity signal was introduced to the central region of a Kanizsa figure, the peak was perceived to lie at an intermediate depth between the relative disparity at the tip of the inducing edge and the luminance-defined disparity at the surface peak (Experiment 4.2). Given that the magnitude of disparity along the vertical surface edge was equivalent in the combined and low contrast conditions, this result seems counterintuitive. Importantly, given that the surfaces were generated using perspective projection, the reduction in perceived depth in the combined surface was not likely due to conflict between the disparity signal and 2D occlusion geometry (see Section 1.6.2). In spite of this, the addition of a luminance signal in the central region of a stereoscopic Kanizsa figure reduced the height of the perceived peak relative to the luminance-defined peak disparity.

A critical difference between the combined and illusory surface configurations was that all T-junctions in the combined surface were explicitly defined by a change in luminance, while the T-junctions in the latter were illusory. Thus, unlike the illusory surface, the edge of the T-junction at the tip of the inducing edge (and surface peak) was no longer ambiguous. The

perceived depth of the combined surface reflects the combination of the occlusion features at the tip of the inducing edge, the disparity signal along the vertical surface edge, and the luminance in the central region. The disparity signal was the only quantitative depth information, in this configuration, the addition of luminance in the central region (like the occlusion features) provided additional qualitative information regarding the sign of depth (Gilchrist, 1977; Gilchrist, 1980). The depth estimates of the surface peak in Experiment 4.2 confirm that a surface defined by the above combination of depth cues has a reduced depth compared to the luminance-defined disparity present at the surface peak. While estimates of the low contrast surface peak without the inducing elements (defined by disparity and luminance only) were equivalent to the peak disparity, the addition of the inducing elements behind the surface significantly reduced the perceived location of the peak. One or more of the occlusion features at the inducing elements appeared to interact with the disparity signal along the surface edge.

6.4.2 Luminance, Occlusion, and Disparity

While the reduction in perceived depth in the combined surface likely relied on similar occlusion and disparity relationships that lead to the generation of illusory boundaries, the impact of the occlusion geometry at the inducers on the perceived disparity at the surface peak could have scaled with the luminance relationships at image junctions (Adelson, 1993). As discussed in Chapter 2, the effects of luminance contrast on stereoscopic thresholds are well established (Frisby & Mayhew, 1978; Legge & Gu, 1989; Ogle & Weil, 1958). However, these factors do not necessarily affect suprathreshold depth estimates in the same manner (Patel, Bedell, Tsang, & Ukwade, 2009; Schor & Howarth, 1986). Previous studies demonstrate that lowering the luminance contrast at a given disparity can cause the object to appear more distant (Fry, Bridgman, & Ellerbrock, 1949; Rohaly & Wilson, 1999), and in some cases the magnitude of

perceived depth directly depends on the luminance contrast of the surface (Chen, Chen & Tyler, 2016). In Chapter 2, I demonstrated that when the contrast of a luminance-defined surface (1.7%) was near contrast threshold, observers did not perceive a coherent stereoscopic illusory surface. However, when the contrast was doubled (3.3%) a stable 3D surface was perceived. As long as the contrast of the surface relative to the background luminance was above this value, the perceived location of the peak of the luminance-defined surface was equivalent to the luminance-defined disparity at the surface peak (low and high contrast surfaces in Experiment 4.2). Luminance and disparity interact over a range of low-luminance values, but as soon as the luminance contrast reaches a given level (suprathreshold) the 3D surface percept was veridical; thus, further increases in luminance provide no additional benefit.

Anderson (2003) suggested that the luminance relationships at depth discontinuities (i.e. occlusions) could impact the interpolation of depth across ambiguous regions (Wurger & Landy, 1989). Previous research has demonstrated in configurations with disparity-defined elements of varying luminance, perceived depth tends to be biased in the direction of the surface with the higher contrast (Foley, 1976; Foley & Richards, 1977; Rohaly & Wilson, 1999). In addition, when multiple disparity-defined plaid surfaces are overlaid in depth, luminance contrast can act as an ordinal depth cue, with higher contrast gratings appearing in front of low contrast gratings (Stoner & Albright, 1998). The high contrast luminance patterns may enhance perceived depth by improving localization of sparse elements and facilitating binocular correspondence.

It is possible that the local contrast signals along the vertical surface edge in the combined Kanizsa configurations influenced the interpolation of depth within the central region. In the combined surface, the vertical surface edge had a region of high contrast at the inducing edge and a region of low contrast between adjacent inducers. The high contrast inducing region had smaller disparities than the region of low contrast. If the higher contrast region of the surface

edge was given more weight than the low contrast region, the resulting combination would be reduced compared to the luminance-defined disparity at the surface peak.

6.5 Conclusions

The results of this series of experiments demonstrate that qualitative depth cues, such as 2D occlusion features and luminance relationships, critically impact estimates of metric depth from binocular disparity. Previous investigations of depth processing have emphasized the role of ordinal depth cues on depth from binocular disparity (Bertamini, Martinovic, & Wuerger, 2008; Burge, Peterson, & Palmer, 2005); the experiments reported here are the first systematic evaluation of the accuracy and precision of suprathreshold depth estimation in stereoscopic illusory surfaces. The assessment of suprathreshold depth estimates allowed this work to be evaluated in the context of a cue combination paradigm. Further evaluation is needed to appropriately model the combination of qualitative (occlusion and luminance) and quantitative (stereopsis) cues to depth in ambiguous configurations. I demonstrated that the 2D border-ownership derived from occlusion features and disparity ownership determine subsequent figure-ground relationships in three-dimensional space. Future experiments will build on these results by systematically exploring how the relationship between the occlusion and luminance features at junctions affect the interpolation of depth across the central region in a cue combination paradigm. The current results support growing evidence that 2D occlusion features contribute rich information about three-dimensional surface structure by influencing perceived depth from binocular disparity.

References

Adelson, E.H. (1993). Perceptual organization and the judgement of brightness. *Science,* 262, 2042-2044.

Albert, M.K. (2001). Surface perception and the generic view principle. *Cognitive Sciences*, *5*(5), 197-203.

Albert, M.K. & Hoffman, D.D. (2000). The generic-viewpoint assumption and illusory contours. *Perception, 29*, 303-312.

Anderson, B.L. (1997). A theory of illusory lightness and transparency in monocular and binocular images: The role of contour junctions. *Perception,* 26, 419-453.

Anderson, B.L. (2003). The role of occlusion in the perception of depth, lightness, and opacity. *Psychological Review,* 110(4), 785-801.

Anderson, B.L. (2007). The demise of the identity hypothesis and the insufficiency and nonnecessity of contour relatability in predicting object interpolation: Comment on Kellman, Garrigan, and Shipley (2005). *Psychological Review,* 114(2), 470-487.

Anderson, B.L. & Julesz, B. (1995). A theoretical analysis of illusory contour formation in stereopsis. *Psychological Review,* 102, 705-743.

Anderson, B.L., Singh, M., & Fleming, R.W. (2002). The interpolation of object and surface structure. *Cognitive Psychology,* 44, 148-190.

Ashley, M.L. (1898). Concerning the significance of intensity of light in visual estimates of depth. *Psychological Review,* 5(6), 595-615.

Banks, M.S., Hooge, I.T.C., Backus, B.T. (2001). Perceiving slant about a horizontal axis from stereopsis. *Journal of Vision,* 1(2), 55-79.

Banton, T. & Levi, D.M. (1992). The perceived strength of illusory contours. *Perception & Psychophysics, 52*(6), 676-684.

Benjamini, Y. & Hochberg, Y. (1995). Controlling the False Discovery Rate: a Practical and Powerful Approach to Multiple Testing. *Journal of the Royal Statistical Society Series B, 57,* 289-300.

Bertamini, M., Martinovic, J., & Wuerger, S.M. (2008). Integration of ordinal and metric cues in depth processing. *Journal of Vision, 8*(2), 1-12.

Blakemore, C. (1970). The range and scope of binocular depth discrimination in man. *Journal of Physiology, 211*, 599-622.

Bradley, D.R., & Dumais, S.T. (1984). The effects of illumination level and retinal size on the depth stratification of subjective contour figures. *Perception, 13,* 155-164.

Brainard, D.H. (1997). The Psychophysics Toolbox. *Spatial Vision, 10*(4), 433-436.

Brenner, E. & van Damme, W.J.M. (1999). Perceived distance, shape and size. *Vision Research, 39,* 975-986.

Brussel, E.M., Stober, S.R., & Bodinger, D.M. (1977). Sensory information and the subjective contour. *American Journal of Psychology, 90,* 145-156.

Burge, J., Peterson, M.A., & Palmer, S.E. (2005). Ordinal configural cues combine with metric disparity in depth perception. *Journal of Vision, 5*, 534-542.

Carman, G.J. & Welch, L. (1992). Three-dimensional illusory contours and surfaces. *Nature,* 360, 585-587.

Cavanagh, P. (1987). Reconstructing the third dimension: Interactions between color, texture, motion, binocular disparity, and shape. *Computer Vision, Graphics, and Image Processing, 37*, 171-195.

Chen, P., Chen, C., & Tyler, C.W. (2016). Perceived depth from disparity depends on luminance contrast. Poster presented at the annual Vision Science Society meeting, St. Pete Beach, FL.
Cochran, W.G. (1937). Problems arising in the analysis of a series of similar experiments. *Journal of the Royal Statistical Society, 4,* 102-118.
Cohen, J. (1988). Stastical power analysis for the behavioral sciences (2nd ed.). Hillsdale, NJ: Lawrence Erlnaum.
Coren, S. (1972). Subjective contours and apparent depth. *Psychological Review,* 79(4), 359-367.
Coren, S. & Porac, C. (1983). Subjective contours and apparent depth: A direct test. *Perception & Psychophysics,* 33, 197-200.
Coules, J. (1955). Effect of photometric brightness on judgments of distance. *Journal of Experimental Psychology,* 50(1), 19-25.
Day, R.H. (1987). Cues for edge and the origin of illusory contours: An alternative approach. In S. Petry & G.E. Meyer (Eds.), *The perception of illusory contours* (pp. 53-61). New York: Springer-Verlag.
Dresp, B., Lorenceau, J., & Bonnet, C. (1990). Apparent brightness enhancement in the Kanizsa square with and without illusory contour formation. *Perception, 19*(4), 483-489.
Dresp, B. (1992). Local brightness mechanisms sketch out surfaces but do not fill them in: Psychophysical evidence in the Kanizsa square. *Perception & Psychophysics, 52,* 562-570.
Ehrenstein, W. (1941). Über Abwandlungen der L. Hermannschen Helligkeitserscheinung. Zeitschrift für Psychologie, *150,* 83-91.
Ehrenstein, W.H. & Gillam, B.J. (1999). Early demonstrations of subjective contours, amodal completion, and depth from half-occlusions: "Stereoscopic experiments with silhouettes" by Adolf von Szily. *Perception,* 27, 1407-1416.
Ernst, M.O. & Banks, M.S. (2002). Humans integrate visual and haptic information in a statistically optimal fashion. *Nature,* 415(24), 429-433.
Fahle, M. & Palm, G. (1991). Perceptual rivalry between illusory and real contours. *Biological Cybernetics,* 66, 1-8.
Farne, M. (1977). Brightness as an indicator to distance: Relative brightness per se or contrast with the background? *Perception,* 6, 287-293.
Foley, J.M. (1976). Binocular depth mixture. *Vision Research, 16,* 1263-1267.
Foley, J. M., Applebaum, T. H., & Richards, W. A. (1975). Stereopsis with large disparities: discrimination and depth magnitude. *Vision Research, 15,* 417-421.
Foley, J.M. & Richards, W.A. (1977). Binocular depth mixture with non-symmetric disparities. *Vision Research, 18,* 251-256.
Frisby, J.P. & Mayhew, J.E.W. (1978). Contrast sensitivity function for stereopsis. *Perception, 7,* 423-429.
Fry, G.A., Bridgman, C.S., & Ellerbrock, V.J. (1949). The effect of atmospheric scattering on binocular depth. *Am J Optom Arch Am Acad Optom, 29,* 9-15.
Gilchrist, A. (1977). Perceived lightness depends on perceived spatial arrangement. *Science,* 195, 185-187.
Gilchrist, A. (1980). When does perceived lightness depend on perceived spatial arrangement. *Perception & Psychophysics,* 28, 527-538.
Gillam, B. (1987). Perceptual grouping and subjective contours. In S. Petry & G.E. Meyer (Eds.), *The perception of illusory contours* (pp. 268-273). New York: Springer-Verlag.

Gillam, B., & Nakayama, K. (2002). Subjective contours at line terminations depend on scene layout analysis, not image processing. *Journal of Experimental Psychology: Human Perception and Performance,* 28, 43-53.
Glennerster, A., McKee, S.P., & Birch, M.D. (2002). Evidence for surface-based processing of binocular disparity. *Current Biology,* 12, 825-828.
Gold, J.M., Murray, R.F., Bennett, P.J., & Sekuler, A.B. (2000). Deriving behavioural receptive fields for visually completed contours. *Current Biology,* 10(11), 662-666.
Gregory, R.L. & Harris, J.P. (1974). Illusory contours and stereo depth. *Perception & Psychophysics,* 15(3), 411-416.
Grimson, W.E.L. (1981). *From images to surfaces: a computational study of the human early visual system.* Cambridge: MIT Press.
Grossberg, S. & Mingolla, E. (1985). Neural dynamics of form perception: Boundary completion, illusory figures, and neon color spreading. *Psychological Review, 92*(2), 173-211.
Grossberg, S., & Yazdanbakhsh, A. (2005). Laminar cortical dynamics of 3D surface perception: Stratification, transparency, and neon color spreading. *Vision Research, 45,* 1725-1743.
Halpern, D.F. (1981). The determinants of illusory-contours perception. *Perception, 10,* 199-213.
Hakkinen, J., Liinasuo, M., Kojo, I., & Nyman, G. (1998). Three-dimensionally slanted illusory contours capture stereopsis. *Vision Research, 38,* 3109-3115.
Harris, J.P. & Gregory, R.L. (1973). Fusion and rivalry of illusory contours. *Perception,* 2(2), 235-247.
He, Z.J., & Ooi, T.L. (1998). Illusory-contour formation affect by luminance contrast polarity. *Perception,* 27(3), 313-335.
Helmholtz, H.V. (1909). Handbuch der physiologischen Optik. *Hamburg: Voss.*
Hillis, J.M., Watt, S.J., Landy, M.S., & Banks, M.S. (2004). Slant from texture and disparity cues: Optimal cue combination. *Journal of Vision, 4,* 967-992.
Howard, I. P. (1995). *Binocular Vision and Stereopsis*: Oxford University Press.
Howard, I.P. & Rogers, B.J. (2012). Perceiving in depth: Volume 2, Stereoscopic vision. Oxford: Oxford University Press.
Johnston, E.B. (1991). Systematic distortions of shape from stereopsis. *Vision Research, 31,* 1351-1360.
Jones, J. & Malik, J. (1992). A computational framework for determining stereo correspondence from a set of linear spatial filters. *Image and Vision Computing,* 10, 699-708.
Jory, M.K. & Day, R.H. (1979). The relationship between brightness contrast and illusory contours. *Perception, 8,* 3-9.
Julesz, B. (1971). *Foundations of cyclopean.* Chicago: University of Chicago Press.
Kanizsa, G. (1955). Margini quasi-percettivi in campi con stimolazione omogenea. *Rivista di Psicologia, 49,* 7-30.
Kanizsa, G. (1974). Contours without gradients or cognitive contours? *Italian Journal of Psychology, 1,* 93-112.
Kanizsa, G. (1976). Subjective contours. *Scientific American,* 234(4), 48-52.
Kanizsa, G. (1979). *Organization in vision*. Praeger: New York.
Kellman, P.J. & Shipley, T.F. (1991). A theory of visual interpolation in object perception. *Cognitive Psychology,* 23, 141-221.
Kellman, P.J., Garrigan, P., & Shipley, T.F. (2005). Object interpolation in three dimensions. *Psychological Review,* 112(3), 586-609.
Knill, D.C., & Kersten, D. (1991). Apparent surface curvature affects lightness perception. *Nature,* 351, 228-230.

Knill, D.C. & Saunders, J. (2002). Humans optimally weight stereo and texture cues to estimate surface slant. *Journal of Vision, 2*(7), 400.
Knill, D.C. & Saunders, J.A. (2003). Do humans optimally integrate stereo and texture information for judgements of surface slant? *Vision Research, 43*, 2539-2558.
Kogo, I., Liinasuo, M., & Rovamo, J. (1993). Spatial and temporal properties of illusory figures. *Vision Research, 33*, 897-901.
Kogo, N., Strecha, C., Gool, L.V., & Wagemans, J. (2010). Surface construction by a 2-D differentiation-integration process: A neurocomputational model for perceived border ownership, depth, and lightness in Kanizsa figures. *Psychological Review*, 117(2), 406-439.
Kogo, N., Drozdzewska, A., Zaenen, P., Alp, N., & Wagemans, J. (2014). Depth perception of illusory surfaces. *Vision Research*, 96, 53-64.
Landy, M.S., Maloney, L.T., Johnston, E.B., & Young, M. (1995). Measurement and modeling of depth cue combination: In defense of weak fusion. *Vision Research, 35*, 389-412.
Larsson, J., Amunts, K., Gulyas, B., Malikovic, A., Zilles, K., Roland, P. (1999). Neuronal correlates of real and illusory contour perception: functional anatomy with PET. *European Journal of Neuroscience,* 11, 4024-4036.
Lawson, R.B., Cowen, E., Gibbs, T.D., & Whitmore, C.G. (1974). Stereoscopic enhancement and erasure of subjective contours. *Journal of Experimental Psychology,* 103, 1142-1146.
Lee, T.S. & Mumford, D.B. (2003). Hierarchical Bayesian inference in the visual cortex. Journal of the Optical Society of America. 20(7), 1434-1448.
Lee, T.S. & Nguyen, M. (2001). Dynamics of subjective contour formation in the early visual cortex. *Proc. Natl. Acad. Sci. USA*, 98, 1907-1911.
Legge G.E. & Gu, Y. (1989). Stereopsis and contrast. *Vision Research, 29*, 989-1004.
Lesher, G.W. (1995). Illusory contours: Toward a neutrally based perceptual theory. *Psychonomic Bulletin & Review, 2*(3), 279-321.
Levitt, H. (1970). Transformed up-down methods in psychoacoustics. *Journal of the Acoustical Society of America, 49*(2), 467-477.
Li, C. & Guo, K. (1995). Measurements of geometric illusions, illusory contours and stereo-depth at luminance and colour contrast. *Vision Research, 35*(12), 1713-1720.
Marr, D. & Poggio, T. (1976). Cooperative computation of stereo disparity. *Science, 194*(4262), 283-287.
Matthews, N. & Welch, L. (1997). The effect of inducer polarity and contrast on the perception of illusory figures. *Perception, 26*(11), 1431-1443.
McKee, S.P., Levi, D.M., & Bowne, S.F. (1990). The imprecision of stereopsis. *Vision Research, 30*, 1763-1779.
McKee, S.P., Welch, L., Taylor, D.G., & Browne, S.F. (1990). Finding the common bond: Stereoacuity and the other hyperacuities. *Vision Research, 22*, 449-460.
Mendola, J.D., Dale, A.M., Fischl, B., Liu, A.K., & Tootell, R.B.H. (1999). The representation of illusory and real contours in human cortical visual areas revealed by functional magnetic resonance imaging. *Journal of Neuroscience,* 19, 8560-8572.
Michotte, A. (1963). *The perception of causality.* New York: Basic Books.
Mitchison, G.J. & McKee, S.P. (1985). Interpolation in stereoscopic matching. *Nature, 315,* 402-404.
Mitchison, G.J. & McKee, S.P. (1987a). The resolution of ambiguous stereoscopic matches by interpolation, *Vision Research,* 27(2), 285-294.

Mitchison, G.J. & McKee, S.P. (1987b). Interpolation and the detection of fine structure in stereoscopic matching. *Vision Research*, 27(2), 295-302.
Mitchison, G.J. & Westheimer, G. (1984). The perception of depth in simple figures. *Vision Research, 24*, 1063-1073.
Nakayama, K., Shimojo, S., & Silverman, G.H. (1989). Stereoscopic depth: Its relation to image sementation, grouping, and the recognition of occluded objects. *Perception,* 18(1), 55-68.
Nakayama, K. & Shimojo, S. (1992). Experiencing and perceiving visual surfaces. *Science,* 257(5075), 1357-1363.
Ogle, K. N. (1952). On the limits of stereoscopic vision. *Journal of Experimental Psychology, 44*(4), 253–259.
Ogle, K. N. (1953). Precision and validity of stereoscopic depth perception from double images. *Journal of the Optical Society of America, 43*(10), 906-913.
Ogle, K.N. & Weil, M.P. (1958). Stereoscopic vision and the duration of the stimulus. *Arch Ophthal, 59*, 4-17.
Ogle, K. N. (1964). *Researches in Binocular Vision*: Hafner.
Oruç, I., Maloney, L.T., & Landy, M.S. (2003). Weighted linear cue combination with possibly correlated error. *Vision Research, 43*, 2451-2468.
Paradiso, M.A., Shimojo, S. & Nakayama, K. (1989). Subjective contours, tilt aftereffects, and visual cortical organization. *Vision Research,* 29, 1205-1213.
Patel, S.S., Bedell, H.E., Tsang, D.K., Ukwade, M.T. (2009). Relationship between threshold and suprathreshold perception of position and stereoscopic depth. *J. Opt. Soc. Am., 26*(4), 847-861.
Pelli, D.G. (1997). The VideoToolbox software for visual psychophysics: transforming numbers into 632 movies. *Spatial Vision, 10*(4), 437-442.
Petry, S., Harbeck, A., Conway, J., & Levey, J. (1983). Stimulus determinants of brightness and distinctness of subjective contours. *Perception & Psychophysics, 34*, 169-174.
Prazdny, K. (1983). Illusory contours are not caused by simultaneous brightness contrast. *Perception and Psychophysics*, 34(4), 403-404.
Qiu, F.T. & von der Heydt, R. (2005). Figure and ground in the visual cortex: V2 combines stereoscopic cues with Gestalt rules. *Neuron, 47*, 155-166.
Ramachandran, V.S. (1986). Capture of stereopsis and apparent motion by illusory contours. *Perception & Psychophysics,* 39, 361-373.
Rashbass. C. & Westheimer, G. (1961). Disjunctive eye movements. *Journal of Physiology, 159,* 339-360.
Reynolds, R.I. (1981). Perception of an illusory contour as a function of processing time. *Perception, 10*, 107-115.
Ringach, D. & Shapley, R. (1996). Spatial and temporal properties of illusory contours and amodal boundary completion. Vision Research, 36(19), 3037-3050.
Roelfsema, P.R., Lamme, V.A., & Spekreijse, H. (1998). Object-based attention in the primary visual cortex of the macaque monkey. *Nature,* 395, 376-381.
Rohaly, A.M., Wilson, H.R. (1999). The effects of contrast on perceived depth and depth discrimination. *Vision Research, 39*, 9-18.
Ross, W.D., Grossberg, S. & Mingolla, E. (2000). Visual cortical mechanisms of perceptual grouping: Interacting layers, networks, columns, and maps. *Neural Network, 13*, 571-588.
Rubin, N. (2001). The role of junctions in surface completion and contour matching. *Perception,* 30, 339-366.

Schor, C.M. & Howarth, P.A. (1986). Suprathreshold stereo-depth matches as a function of contrast and spatial frequency. *Perception, 15*(3), 249-258.
Schumann, F. (1900). Beitrage zur analyse der Gesichtswahrnehmungen. *Zeitschrift fur Psychologie und Physiologie der Sinnesorgane,* 23, 1-32.
Shapley, R. (1996). Art and perception of nature: Illusory contours in the paintings of Ellsworth Kelly. *Perception, 25*, 1259-1261.
Shipley, T.F. & Kellman, P.J. (1990). The role of discontinuities in the perception of subjective figures. *Perception & Psychophysics*, 48, 259-270.
Shipley, T.F. & Kellman, P.J. (1992). Strength of visual interpolation depends on the ratio of physically specified to total edge length. *Perception and Psychophysics*, 52(1), 97-106.
Singh, M. & Hoffman, D.D. (1999). Completing visual contours: The relationship between relatability and minimizing inflections. *Perception & Psychophysics, 61*, 943-951.
Smith, A.T. & Over, R. (1979). Motion aftereffect with subjective contours. *Perception & Psychophysics*, 25, 95-98.
Spillman, L.A., Fuld, K., & Neumeyer, C. (1984). Brightness matching, brightness cancellation, and increment threshold in the Ehrenstein illusion. *Perception, 13*, 513-520.
Stanley, D.A. & Rubin, N. (2003). fMRI activation in response to illusory contours and salient regions in the human lateral occipital complex. *Neuron*, 37, 323-331.
Stevens, Kent, Lees, Marek, & Brookes, Allen (1991). Combining binocular and monocular curvature features. *Perception, 20*, 425-440.
Stoner, G.R. & Albright, T.D. (1998). Luminance contrast affects motion coherency in plaid patterns by acting as a depth-from-occlusion cue. *Vision Research, 38*(3), 387-401.
Taylor, I.L. & Sumner, F.C. (1945). Actual brightness and distance of individual colors when their apparent distance is held constant. *Journal of Psychology*, 19(1), 79-85.
Tse, P. & Albert, M. (1998). Amodal completion in the absence of image tangent discontinuities. *Perception*, 27, 455-464.
Tulunay-Keesey, U. & Jones, R.M. (1976). The effect of micromovements of the eye and exposure duration on contrast sensitivity. *Vision Research, 16*, 481-488.
Ullman, S. (1976). Filling-in the gaps: The shape of subjective contours and a model for their generation. *Biol. Cybernetics, 25*, 1-6.
VanRullen, R. & Thorpe, S. (2001). Is it a bird? Is it a plane? Ultra-rapid visual categorization of natural and artificial objects. *Perception,* 30, 655-668.
Vogels, R. & Orban, G.A. (1987). Illusory contour orientation discrimination. *Vision Research,* 27, 453-467.
von der Heydt, R., Peterhans, E., & Baumgarthner, G. (1984). Illusory contours and cortical neuron responses. *Science*, 224, 1260-1262.
Vreven, D. & Welch, L. (2001). The absence of depth constancy in contour stereograms. *Perception,* 30, 693-705.
Vreven, D., McKee, S.P., Verghese, P. (2002). Contour completion through depth interferes with stereoacuity. *Vision Research, 42*, 2153-2162.
Watt, S.J., Akeley, K., Ernst, M.O., & Banks, M.S. (2005). Focus cues affect perceived depth. *Journal of Vision, (5)*, 834-862.
Warren, P.A., Maloney, L.T., & Landy, M.S. (2002). Interpolating sampled contours in 3-D: analyses of variability and bias. Vision Research, 42(21), 2431-2446.
Westheimer, G. & Mitchell, D.E. (1969). The sensory stimulus for disjunctive eye movements. *Vision Research, 9*, 749-755.

Westheimer, G. & Li, W. (1997). Classifying illusory contours: Edges defined by “pacman” and monocular tokens. *Journal of Neurophysiology, 77*(2), 731-736.
Wichmann, F. A., & Hill, N. J. (2001a). The psychometric function: I. Fitting, Sampling, and Goodness of fit. *Perception and Psychophysics, 63*(8), 1293-1313.
Wichmann, F. A., & Hill, N. J. (2001b). The psychometric function: II.
Wilcox, L.M. (1999). First and second-order contributions to surface interpolation. *Vision Research,* 39(14), 2335-2347.
Wilcox, L.M & Duke, P.A. (2003). Stereoscopic surface interpolation supports lightness constancy. *Psychological Science,* 14(5), 525-530.
Wilcox, L.M. & Duke, P.A. (2005). Spatial and temporal properties of stereoscopic surface interpolation. *Perception,* 34, 1325-1338.
Wishart, K.A., Frisby, J.P., & Buckley, D. (1997). The role of 3D surface slope in a lightness/brightness effect. *Vision Research,* 37, 467-473.
Wokke, M.E., Vandenbrouche, A., Scholte, S., & Lamme, V. (2013). Confused your illusion: Feedback to early visual cortex contributes to perception completion. *Psychological Science, 24*(1), 63-71.
Wurger, S.M. & Landy, M.S. (1989). Depth interpolation with sparse disparity cues. *Perception, 18,* 39-54.
Yang, Y & Blake, R. (1995). On the accuracy of surface reconstruction from disparity interpolation. *Vision Research,* 35(7), 949-960.
Yang, Q., Bucci, M.P., & Kapoula, Z. (2002). Latency of Saccades, vergence, and combined eye movements in children and in adults. *Investigative Ophthalmology & Visual Science, 43*(9), 2939-2949.
Yin, C., Kellman, P.J., & Shipley, T.F. (2000). Surface integration influences depth discrimination. *Vision Research, 40,* 1969-1978.

Appendices

Appendix A

Table A.1

Individual Diplopia Thresholds from Experiment 2.1

Observer	Diplopia Point (deg)	Lower 95% CI	Upper 95% CI
BH	0.174	0.168	0.18
LD	0.168	0.157	0.178
LW	0.167	0.158	0.176
MC	0.165	0.155	0.175
MG	0.172	0.165	0.18
MJ	0.143	0.135	0.152
AS	0.142	0.134	0.149

Note: Diplopia point represents the relative disparity at the tip of the vertical inducing edge when the probability of an observer perceiving the inducing edge as no longer perceptually fused is 50%.

Appendix B

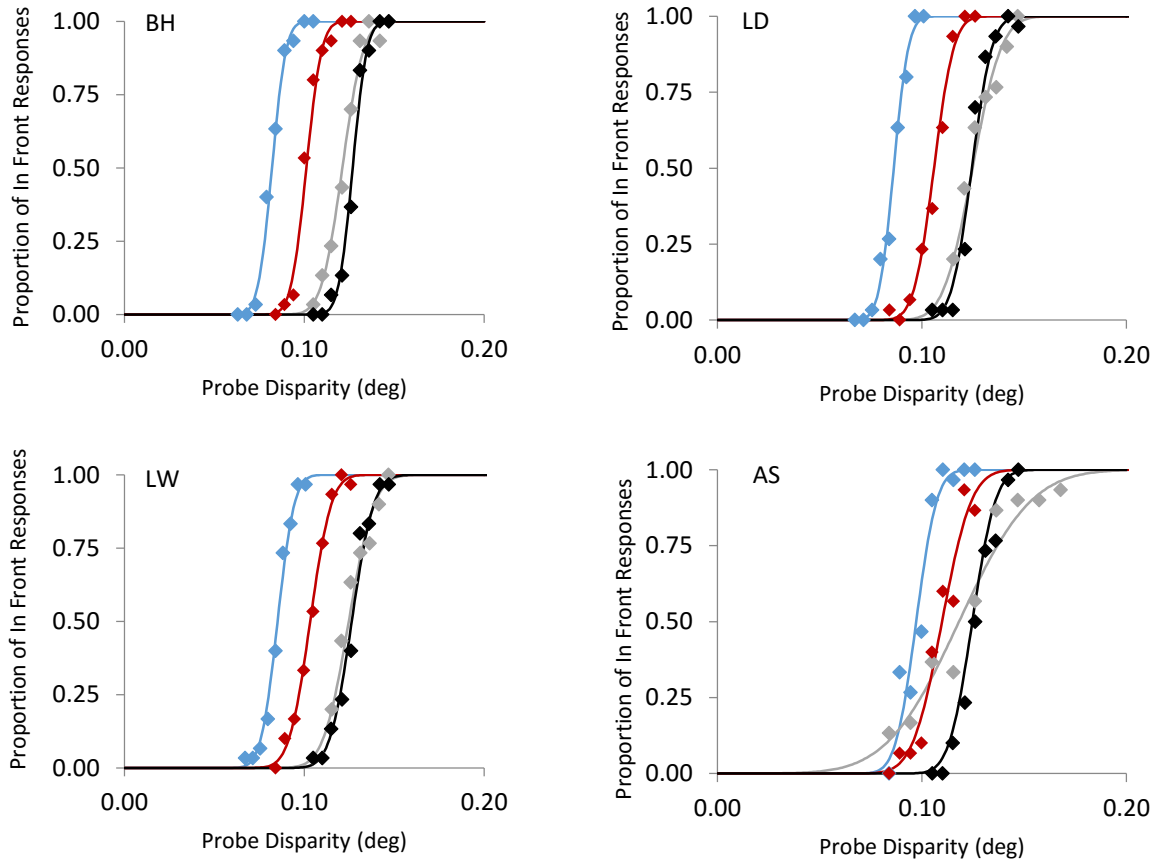

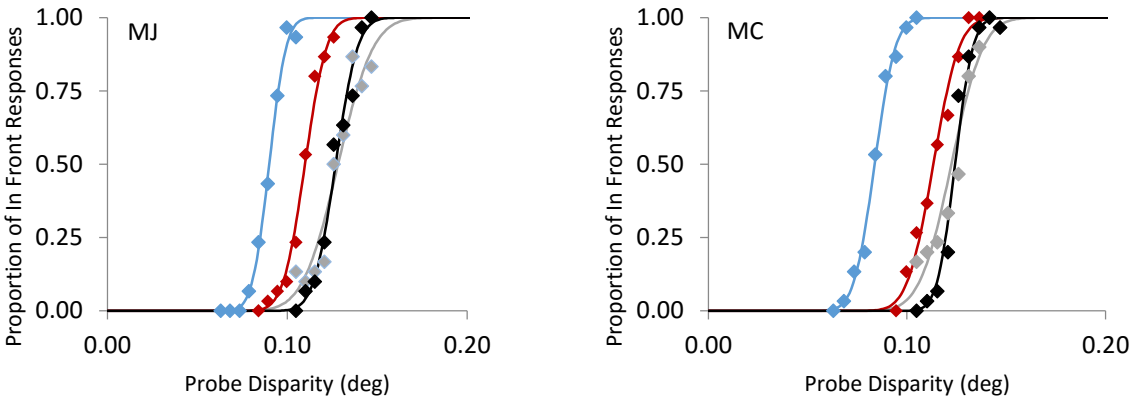

Figure B.1. Individual functions for the High Contrast (black), Low Contrast (grey), Illusory Only (blue), and Combined conditions (red) in the fused range. Each function is plotted as the proportion of in front response as a function of probe disparity in degrees. The PSE of the function represents the estimated disparity of the peak of each type of surface.

Appendix C

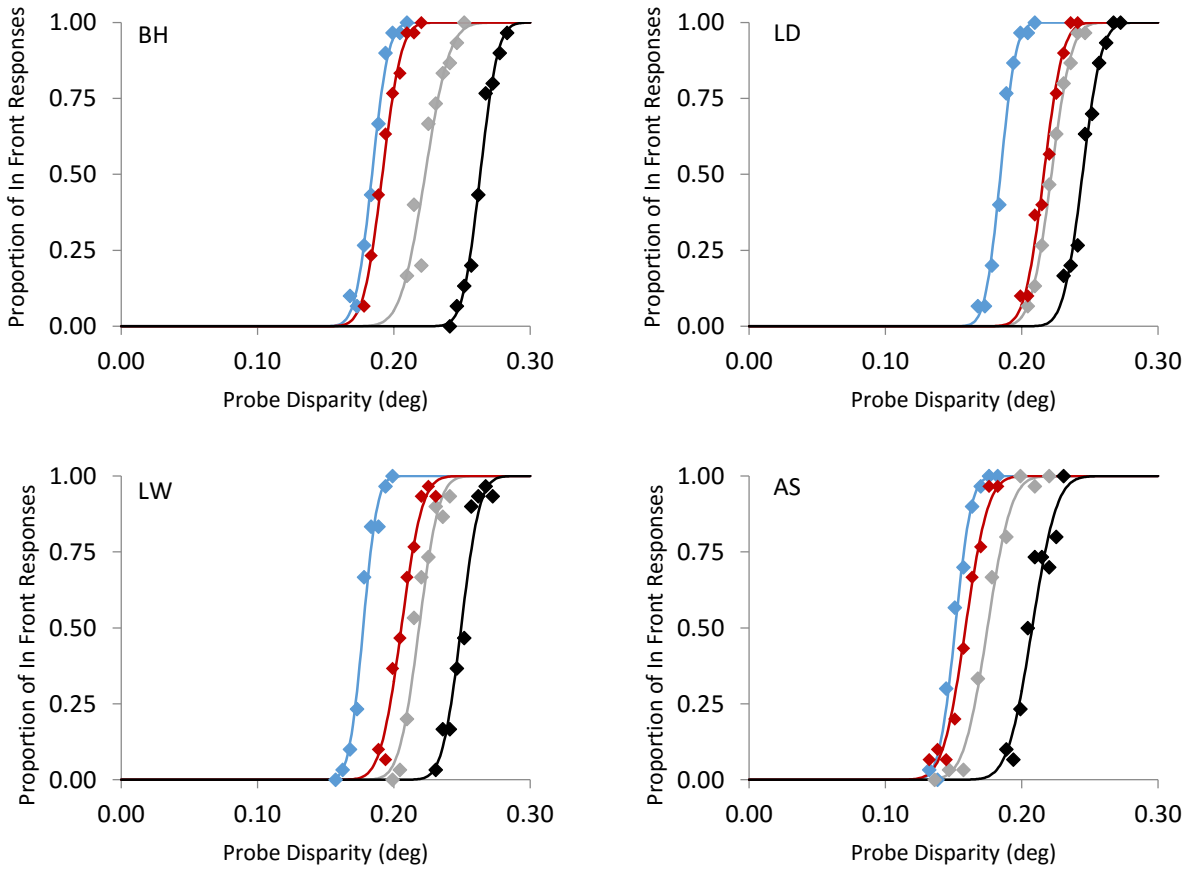

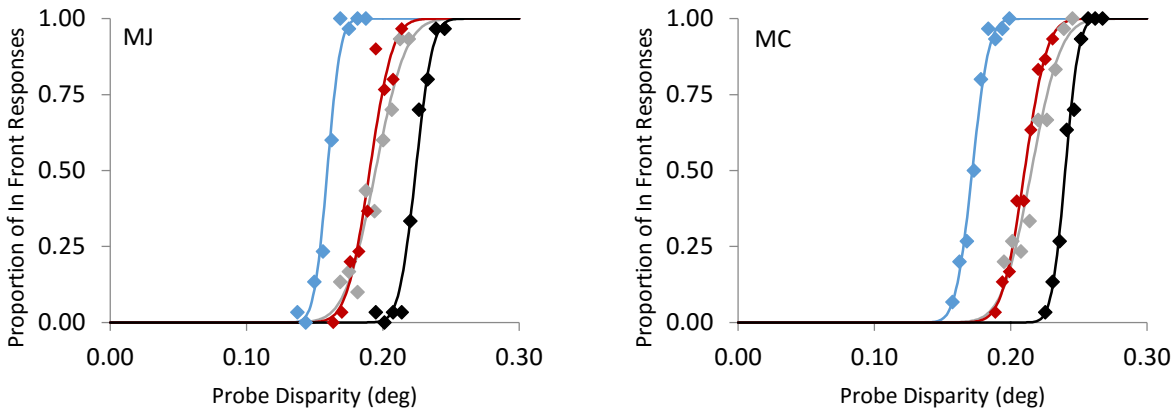

Figure C.1. Individual functions for the High Contrast (black), Low Contrast (grey), Illusory Only (blue), and Combined conditions (red) at the diplopia threshold. Each function is plotted as the proportion of in front response as a function of probe disparity in degrees. The PSE of each function represents the estimated disparity of the surface peak.

Appendix D

Table D.1

Mean Differences in Depth Magnitude and Disparity Probe Tasks

		Depth Magnitude	Disparity Probe	
Comparison	**Observer**	**Mean Diff. (mm)**	**PSE Diff. (deg)**	**PSE Diff. (mm)**
Combined - Illusory Only	BH	-0.64	0.019	3.01
	LD	3.00	0.020	3.17
	AS	-7.30	0.012	1.91
	LW	-0.03	0.018	2.86
	MC	6.24	0.029	4.44
	MJ	0.37	0.020	3.12
Low Contrast - Illusory Only	BH	-1.71	0.039	6.16
	LD	-4.55	0.039	6.16
	AS	-6.32	0.021	3.33
	LW	1.53	0.040	6.32
	MC	1.19	0.038	5.81
	MJ	0.13	0.038	5.91

Note: All values are calculated for a fused surface with an inducer disparity of 0.087deg (i.e. fused standard). Mean Diff. represents the difference between the means of the comparison in the depth magnitude estimation task in millimetres. The PSE Diff. represents the difference between the PSEs in millimetres calculated using the conventional formula relating disparity to predicted depth at a known viewing distance (Howard & Rogers, 2012).